Journal of Paleontology, 95(6), 2021, p. 1113–1137

Published by Cambridge University Press
on behalf of The Paleontological Society
0022-3360/21/1937-2337
doi: 10.1017/jpa.2021.45

JOURNAL OF PALEONTOLOGY
A PUBLICATION OF THE Paleontological SOCIETY

Shale-hosted biota from the Dismal Lakes Group in Arctic Canada supports an early Mesoproterozoic diversification of eukaryotes

Corentin C. Loron,[1] Galen P. Halverson,[2] Robert H. Rainbird,[3] Tom Skulski,[3] Elizabeth C. Turner,[4] and Emmanuelle J. Javaux[1]

[1]Early Life Traces and Evolution–Astrobiology Laboratory, UR Astrobiology, University of Liège, Liège, Belgium <c.loron@uliege.be>, <ej.javaux@uliege.be>
[2]Department of Earth and Planetary Sciences, McGill University, Montreal, Quebec, Canada <galen.halverson@mcgill.ca>
[3]Geological Survey of Canada, Ottawa, Ontario, Canada <rob.rainbird@canada.ca>, <tom.skulski@canada.ca>
[4]Harquail School of Earth Sciences, Laurentian University, Sudbury, Ontario, Canada <eturner@laurentian.ca>

Abstract.—The Mesoproterozoic is an important era for the development of eukaryotic organisms in oceans. The earliest unambiguous eukaryotic microfossils are reported in late Paleoproterozoic shales from China and Australia. During the Mesoproterozoic, eukaryotes diversified in taxonomy, metabolism, and ecology, with the advent of eukaryotic photosynthesis, osmotrophy, multicellularity, and predation. Despite these biological innovations, their fossil record is scarce before the late Mesoproterozoic. Here, we document an assemblage of organic-walled microfossils from the 1590–1270 Ma Dismal Lakes Group in Canada. The assemblage comprises 25 taxa, including 11 morphospecies identified as eukaryotes, a relatively high diversity for this period. We also report one new species, *Dictyosphaera smaugi* new species, and one unnamed taxon. The diversity of eukaryotic forms in this succession is comparable to slightly older assemblages from China and is higher than worldwide contemporaneous assemblages and supports the hypothesis of an earlier diversification of eukaryotes in the Mesoproterozoic.

Introduction

Eukaryotes are an important part of the Precambrian fossil record. Molecular clock calculations estimate the age of the last eukaryotic common ancestor (LECA) to between 1.9 and 1.0 Ga (Parfrey et al., 2011; Eme et al., 2014), and nonambiguous eukaryotic body fossils are reported from 1.65 Ga strata (Javaux et al., 2004; Lamb et al., 2009; Javaux, 2019; Miao et al., 2019).

Although the Proterozoic record of fossil eukaryotes is dominated by organic-walled microfossils, it also preserves macroscopic carbonaceous compressions often interpreted as macroalgae (review in Bykova et al., 2020), but the eukaryotic nature or identity of some is unclear. Organic-walled microfossils from shale and siltstone of the 3.2 Ga Moodies Group in South Africa may represent much older stem eukaryotes, but they lack important diagnostic criteria (e.g., conspicuous surface ornamentation or processes) to distinguish them from prokaryotes (Javaux et al., 2010). A diversification model (Javaux, 2011; Javaux and Lepot, 2018) and paleodiversity data (Knoll et al., 2006; Cohen and Macdonald, 2015; Riedman and Sadler, 2017) indicate that the eukaryotic domain developed various biological innovations during the late Paleoproterozoic–early Mesoproterozoic (review in Javaux, 2007, 2011; Knoll, 2014; Butterfield, 2015a; Cohen and Macdonald, 2015; Javaux and Knoll, 2017; Porter, 2020), such as multicellularity (Butterfield, 2009; Knoll and Lahr, 2016; Javaux and Knoll, 2017), predation (Porter, 2016; Cohen and Riedman, 2018; Loron et al., 2018), and photosynthesis (Butterfield, 2015b), leading to the emergence of major crown groups before the end of the Mesoproterozoic. These views are supported by recent studies of late Mesoproterozoic–Neoproterozoic fossil assemblages (Baludikay et al., 2016; Beghin et al., 2017; Tang et al., 2017; Loron et al., 2019a) and various reports of crown-group eukaryotes, such as probable (Loron et al., 2019b; Berbee et al., 2020) and putative (Berbee et al., 2020; Bonneville et al., 2020) fungi; testate amoebae (Porter and Knoll, 2000; Porter et al., 2003; Morais et al., 2017; Riedman et al., 2018; Martí Mus et al., 2020); red algae (Butterfield, 2000; Gibson et al., 2017); possible and probable green algae (Butterfield et al., 1994, 2015b; Arouri et al., 1999; Marshall et al., 2005; Dong and Xiao, 2006; Moczydłowska and Willman, 2009; Moczydłowska, 2016; Brocks et al., 2017; Tang et al., 2020); possible xanthophyte algae (Butterfield, 2004); foraminifera (Bosak et al., 2011a, b; Brocks et al., 2017); possible ciliates (Bosak et al., 2012); and possible stem metazoan eggs (Cornet et al., 2019). However, the ciliate candidates proposed by Bosak et al. (2012) are reinterpreted as red algal spores by Cohen et al. (2020), and *Jacutianema* (Butterfield, 2004) lacks diagnostic characteristics and falls outside the molecular clock estimates for xanthophyte algae (Butterfield, 2015b). Similarly, the fungal affinity of the filaments reported by Bonneville et al. (2020) are ambiguous (Berbee et al., 2020), and their syngenicity is doubtful.

Although some of those examples have yet failed to find a scientific consensus and need further investigation, the overall record in Mesoproterozoic–Neoproterozoic successions supports the importance of this hinge period for eukaryotic crown-group evolution. All these data suggest that crown-group

eukaryotes may have already been present by the early Mesoproterozoic and were minor, or overlooked, components of paleontological assemblages (Javaux, 2011; Knoll, 2014; Butterfield, 2015a; Javaux and Knoll, 2017; Javaux and Lepot, 2018); alternatively, they may have emerged later, at the end of the Mesoproterozoic, shortly before their diversification (Porter, 2020).

Recent studies of late Paleoproterozoic and early Mesoproterozoic shale-hosted assemblages of the ca. 1.74–1.41 Ga Ruyang Group (Yin et al., 2005; Agić et al., 2015, 2017) and the ca. 1.67–1.63 Ga Changcheng Group (Miao et al., 2019) from China, the ca. 1630 Vindhyan Supergroup from India (Prasad et al., 2005), the ca. 1.49 Ga Roper Group from Australia (Javaux et al., 2001; Javaux and Knoll, 2017), and the ca. 1.58–1.45 Ga lower Belt Supergroup, Montana (Adam et al., 2017) show that microfossils with eukaryotic characteristics were already moderately diverse at that time. However, with 14 eukaryotic taxa recognized in the Beidajian and Baicaoping formations, the Ruyang Group (Agić et al., 2015, 2017) is an exception for a time otherwise marked by a low eukaryotic diversity (≤8 taxa; Prasad et al., 2005; Nagovitsin, 2009; Vorob'eva et al., 2015; Adam et al., 2017; Javaux and Knoll, 2017; Miao et al., 2019). This exceptional assemblage may constitute an example of primary eukaryotic radiation in the late Paleoproterozoic but is, for now, constrained to a particular geographic area (North China craton). Therefore, it is important to document late Paleoproterozoic–early Mesoproterozoic assemblages in other parts of the world.

This paper presents an assemblage of organic-walled microfossils from shales of the Dease Lake and Fort Confidence formations of the Dismal Lakes Group of Arctic Canada. Although microbialites and microfossils were previously recognized and studied in the Dismal Lakes Group (Horodyski and Donaldson, 1980, 1983; Horodyski et al., 1980; Bartley et al., 2015), shales from the Dease Lake and Fort Confidence formations have not yet been investigated. The new assemblage described here presents a moderate diversity of 25 forms, including 11 eukaryotic taxa, one new species, and one as-yet-unnamed taxon. This new example of early Mesoproterozoic eukaryotic diversity, compared with other contemporaneous assemblages, supports that eukaryotic diversification had already begun by the early Mesoproterozoic.

Geological setting

The organic-walled microfossils studied here are extracted from the shale units of the Dismal Lakes Group in northwestern Canada.

Dismal Lakes Group.—The Dismal Lakes Group is exposed in the Coppermine River basin, which straddles the Nunavut–Northwest Territories border of northern mainland Canada (Fig. 1). The Dismal Lakes Group unconformably overlies the Hornby Bay Group, which forms the base of the Hornby Bay sedimentary basin (Ross et al., 1989). It consists of terrestrial to shallow-marine siliciclastic rocks (LeRoux and Fort Confidence formations), which pass up-section into shallow- and deeper-water carbonate rocks (Dease Lake, Kendall River, Sulky, and Greenhorn Lakes formations; Kerans et al., 1981; Fig. 2). The Fort Confidence Formation gradationally overlies the LeRoux Formation and has a maximum thickness exceeding 200 m on the basis of outcrop studies (Kerans, 1983). It is composed of interbedded wavy- and lenticular-bedded sandstone and carbonaceous mudstone, interpreted to represent extensive tidal-flat deposits. The shale samples HB07-41A 183m and HB07-41A 232m, from which most of the fossil specimens were recovered, contain folded sandstone dikelets representing infilled desiccation cracks. This is indicating an intermittent subaerial exposure (see Rainbird et al., 2020).

The Dease Lake Formation is best exposed west of the Dismal Lakes (Fig. 1) where it comprises three members (Kerans, 1982; Ross et al., 1989). Specimens collected for this microfossil study come from the middle member, which consists of cross-laminated sandy dolostone, microbially laminated to stromatolitic dolostone, and dark siltstone (Skulski at al., 2018).

Age of the Dismal Lakes Group.—The depositional age of the Dismal Lakes Group is broadly constrained to between 1590 Ma—the age of mafic sills that intrude the underlying Hornby Bay Group but not the Dismal Lakes Group (U–Pb; Hamilton and Buchan, 2010)—and 1270 Ma, the U–Pb baddeleyite age of Mackenzie diabase dikes that cross-cut the Dismal Lakes Group (LeCheminant and Heaman, 1989; French et al., 2002; Mackie et al., 2009) (Fig. 2). A more specific age of 1438 ± 8 Ma (2σ) was obtained using Re–Os isotope geochronology of finely crystalline pyrite from a shale sample from the Fort Confidence Formation (HB-07-41) (Rainbird et al., 2020). The pyrite probably formed during early diagenesis of the shale, so its age is probably closer to the minimum age than to the maximum age. Because most of the microfossils from this study are reported from the same strata (HB-07-41A), the age of the present assemblage can be constrained between 1446 and 1430 Ma.

Materials and methods

The shale samples analyzed in this study were collected from drill core (uranium exploration core drilled by Unor Inc. in 2007; see Rainbird et al., 2020) and outcrop during a field expedition in summer 2017. Samples were crushed into fine fragments and demineralized by static maceration in hydrochloric and hydrofluoric acids in the Early Life Traces and Evolution–Astrobiology Laboratory of the University of Liège (Belgium) (Early life lab) following a low-manipulation and low-agitation protocol established by Grey (1999). The kerogenous residue obtained from acid treatments was filtered with 25 µm and 10 µm mesh-size filters and mounted on microscope slides. Microfossils were identified, measured, and imaged using an Axio Imager A1m microscope equipped with an AxioCam MRc5 digital camera (Carl Zeiss, Germany) in the Early life lab. Additional smear microscopic slides were prepared for scanning electron microscopy (SEM) and gold-coated using a Quorum q150T ES. Images were acquired using an Auriga microscope (Carl Zeiss, Germany) at the Institut de Physique du Globe de Paris (IPGP), Paris, France.

https://doi.org/10.1017/jpa.2021.45 Published online by Cambridge University Press

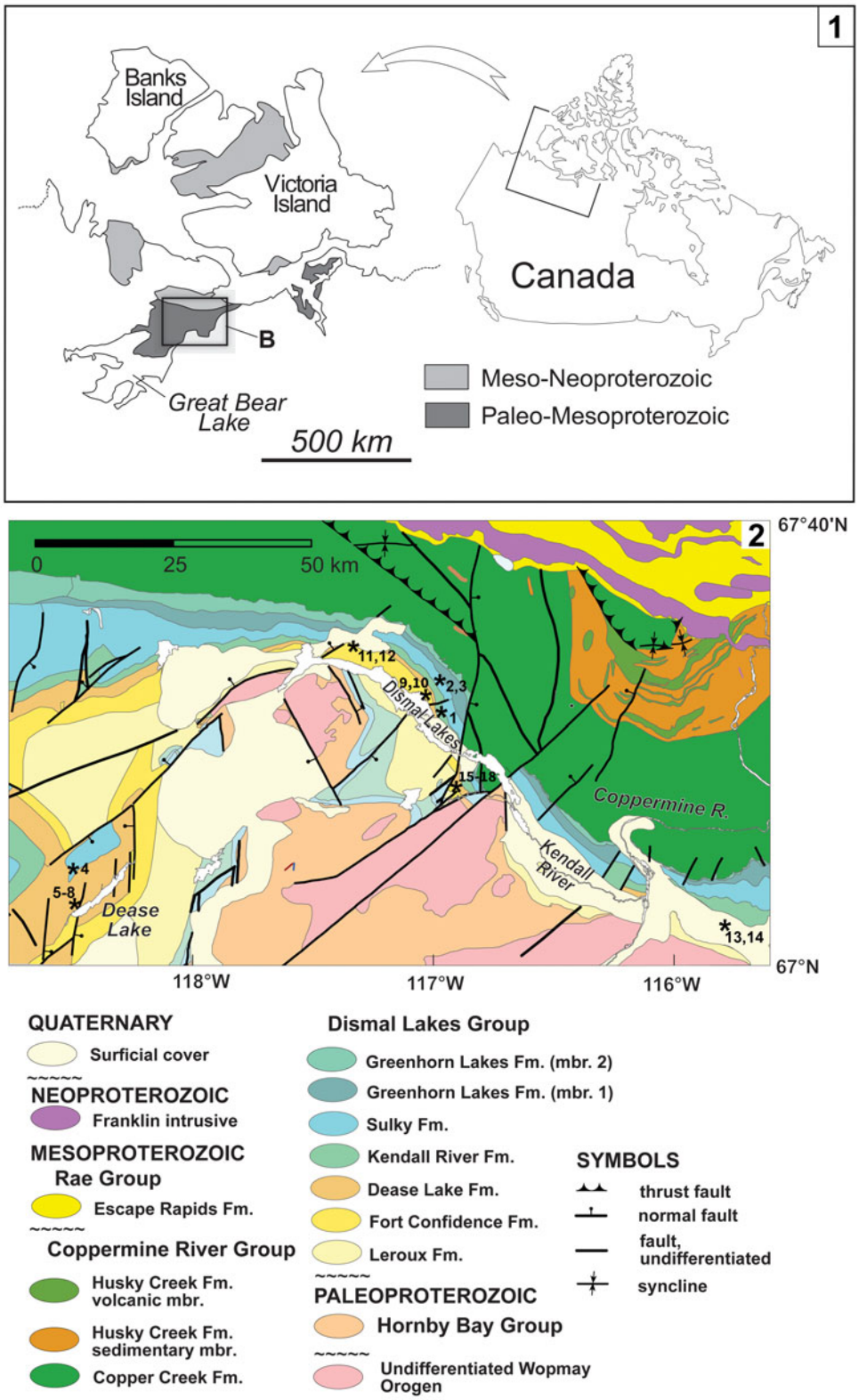

Figure 1. (**1**) Location of study area in northwestern Canada. (**2**) Geological map of the study area. Locations of the samples indicated by asterisks (see table in supplementary data for GPS coordinates); samples 13, 14, 15–18 were extracted from drill core. Modified from Baragar and Donaldson (1973) and Ross et al. (1989).

https://doi.org/10.1017/jpa.2021.45 Published online by Cambridge University Press

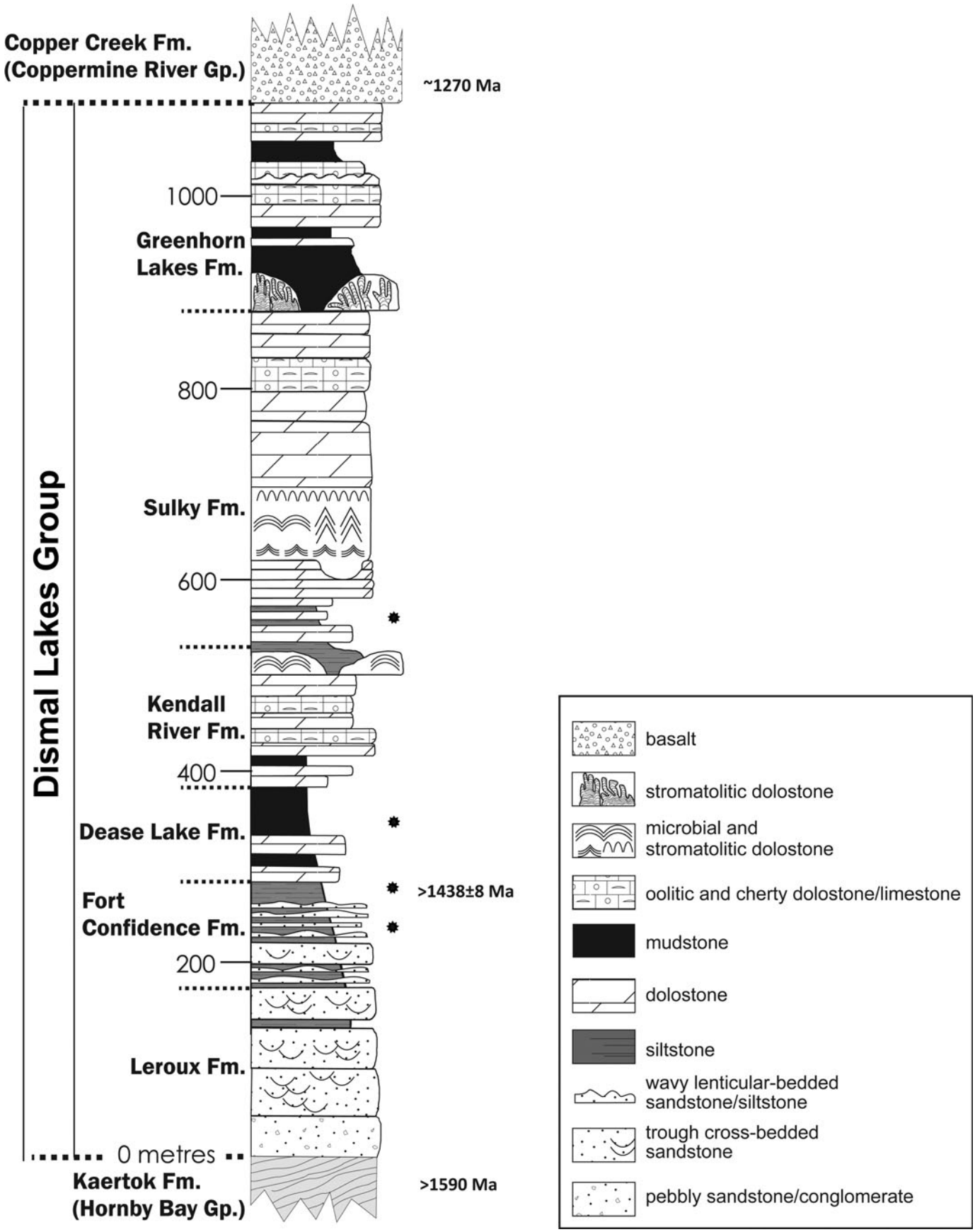

Figure 2. Simplified stratigraphic column for the Dismal Lakes Group, modified from Kerans et al. (1981) and Franck et al. (2003). Black asterisks indicate approximate positions of the sampled strata.

https://doi.org/10.1017/jpa.2021.45 Published online by Cambridge University Press

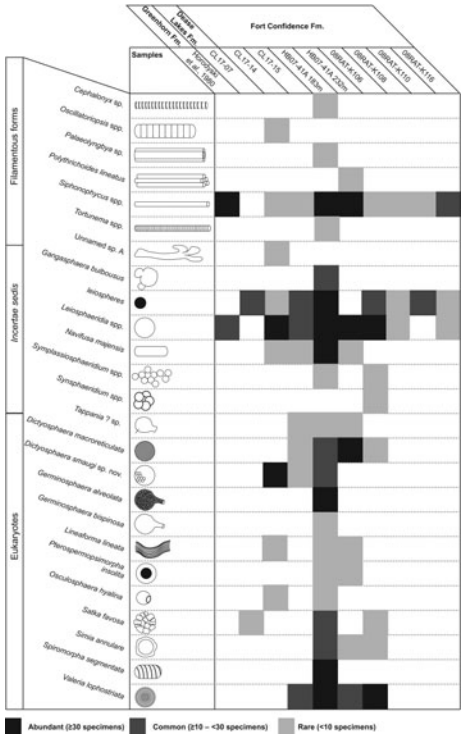

Figure 3. Microfossil distribution in shale of the Dismal Lakes Group, including early work from Horodyski et al. (1980). Note that the highest diversity is in sample HB07-41A 183 m.

Eighteen samples were collected and prepared from the Sulky, Dease Lake, and Fort Confidence formations. With the exception of CL17-12, all samples yielded organic material, though with variable abundances (see Supplementary Table). Nine samples were fossiliferous (eight from the Fort Confidence Formation and one from the Dease Lake Formation; member d1; Fig. 3).

Repository and institutional abbreviation.—All illustrated specimens are identified by slide number—England Finder coordinates and stored in the collection of the Early life lab at the University of Liège, Liège, Belgium (E.J. Javaux).

Systematic paleontology

The microfossils are described following the *International Code of Nomenclature for Algae, Fungi, and Plants* (*Shenzhen Code*; ICBN) (Turland et al., 2018). Taxa conventionally organized in arbitrary size-class species and previously abundantly described in the literature are left under open nomenclature and are discussed in the text (*Siphonophycus* spp.; *Leiosphaeridia* spp., *Oscillatoriopsis* spp., *Tortunema* spp., *Synsphaeridium* spp., *Symplassiosphaeridium* spp.). In the following, we describe 14 taxa interpreted as eukaryotes or possible eukaryotes. Specimens that are morphologically identical but may differ in size are grouped within a single "species." Such species are morpho-species, with no necessarily real biological identity, as usual in paleontology. Some specimens placed in distinct species might represent different developmental stages of a same microorganism, but in absence of complementary analyses, they remain interpreted as separate entities. New genera and species are erected for specimens that show clearly different morphologies from those previously known. The taxa are listed in alphabetical order under the designation "Organic-walled microfossils."

Organic-walled Microfossils

Genus *Dictyosphaera* Xing and Liu, 1973

Type species.—*Dictyosphaera macroreticulata* Xing and Liu, 1973.

Remarks.—The genus was revised by Agić et al. (2015), and the five species *D. macroreticulata*, *D. sinica* Xing and Liu, 1973, *D. delicata* Yin et al., 2005, *D. gyrorugosa* Hu and Fu, 1982, and *D. incrassata* Yan and Zhu, 1992 were synonymized under the type and senior species, *D. macroreticulata*. Subsequently, Tang et al. (2015) described *D. tacita* for vesicles with a smooth external wall and smaller hexagonal plates located on the inner vesicle surface, on the basis of two specimens. The present material contains specimens of *D. macroreticulata* and specimens of *D. smaugi* n. sp. The latter exhibits a wall partially made of polygonal plates, bears no excystment structure, and therefore is distinct from *D. macroreticulata.*

Dictyosphaera macroreticulata Xing and Liu, 1973

Figure 4.7–4.9

1973 *Dictyosphaera macroreticulata* Xing and Liu, p. 22, pl. I16, I17.
2001 *Dictyosphaera* sp.; Javaux et al., p. 67, fig. 1e.
2005 *Dictyosphaera delicata*; Yin et al., p. 52, fig. 2.1, 2.2, 2.5, 2.7, 2.9, 2.10.
2015 *Dictyosphaera macroreticulata*; Agić et al., p. 32, fig. 2.1–2.9.
2017 *Dictyosphaera macroreticulata*; Javaux and Knoll, p. 6, fig. 2.15.
2017 *Dictyosphaera macroreticulata*; Agić et al., p. 108, figs. 3A–F, 4A–C, 14G.
2017 *Dictyosphaera macroreticulata*; Adam et al., p. 388, fig. 3A–C.
2019a *Dictyosphaera macroreticulata*; Loron et al., p. 368, fig. 4M.
2019 *Dictyosphaera macroreticulata*; Miao et al., p. 185, fig. 4a–f.

See Agić et al. (2015) and Miao et al. (2019) for extended synonymy.

Lectotype.—*D. macroreticulata* Xing and Liu, 1973 (pl. 1, fig. 18) from the Chuanlingguo Formation, northern China, Mesoproterozoic. The species was originally described as *Dictyosphaera sinica* Xing and Liu, 1973, junior synonym of *D. macroreticulata* (Agić et al., 2015)

Occurrence.—Paleoproterozoic of the Chuanlinggou Formation, Changcheng Group, China (Xing and Liu, 1973; Miao et al., 2019); Paleoproterozoic–Mesoproterozoic of the Baicaoping and Beidajian formations, Ruyang Group, China

https://doi.org/10.1017/jpa.2021.45 Published online by Cambridge University Press

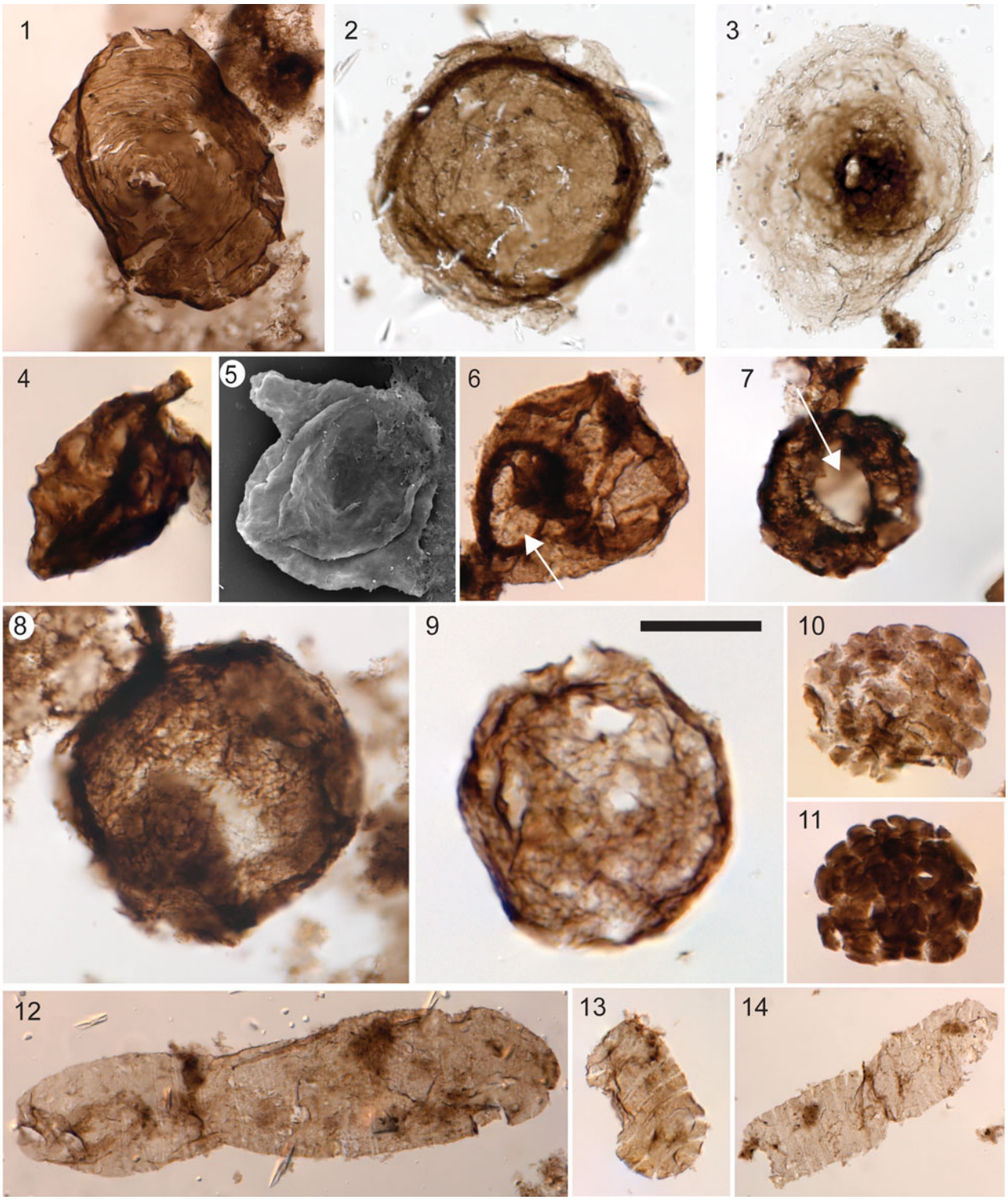

Figure 4. (**1**) *Valeria lophostriata*, 76521-t32, 4. (**2**) *Simia annulare*, 76091-r27. (**3**) *Pterospermopsimorpha insolita*, 76091-v52. (**4, 5**) *Germinosphaera bispinosa*: (**4**) bearing one large process (76801-h28,4); (**5**) bearing two large processes (DLFC-25; SEM). (**6**) *Osculosphaera hyalina*, with a large pylome opening (excystment structure; arrow), 76801-s37,2. (**7–9**) *Dictyosphaera macroreticulata*: (**7**) 76092-n30,1 bearing a pylome opening (arrow); (**8**) 76567-f45; (**9**) 75514-o58. (**10, 11**), *Satka favosa*: (**10**) 76803-u34; (**11**) 76514-m45. (**12–14**) *Spiromorpha segmentata*: (**12**) 76091-j35; (**13**) 76522-f54, 4; (**14**) 76511-y41. All photomicrographs taken under transmitted, plane-polarized light. (**1–7, 9–14**) are from sample HB07-41A 183 m; (**8**) is from sample HB07-41A 232 m. Scale bar in (**9**) = 20 μm for (**4, 5, 9–11, 13**), 30 μm for (**1–3, 6, 8, 12**), 40 μm for (**7**), and 50 μm for (**14**).

(Yin et al., 2005; Agić et al., 2015, 2017); Mesoproterozoic of the Velkerri Formation, Roper Group, Australia (Javaux et al., 2001; Javaux and Knoll, 2017); Mesoproterozoic Greyson Formation, Belt Supergroup, Montana (Adam et al., 2017); Mesoproterozoic of the Fort Confidence Formation, Dismal Lakes Group, Canada (this study); and late Mesoproterozoic–

https://doi.org/10.1017/jpa.2021.45 Published online by Cambridge University Press

early Neoproterozoic Escape Rapids and Grassy Bay formations, Shaler Supergroup, Canada (Loron et al., 2019a). See Agić et al. (2015) for extended occurrences.

Description.—Spheroidal vesicles, 37.5 to 132.5 µm in diameter (n = 13). The wall is composed of >1 µm tessellate polygonal platelets. Excystment structure (pylome) is present on one specimen (11.9 µm in diameter).

Materials.—Fifty-five specimens in sample CL17-15, HB07-41A 183 m, HB07-41A 232 m, and 08RAT-K106.

Remarks.—Although *D. macroreticulata* is interpreted as a taxon characteristic of Mesoproterozoic rocks (Javaux et al., 2001; Agić et al., 2015, 2017; Adam et al., 2017; Javaux and Knoll, 2017), it has recently been reported from the <1013–892 ± 13 Ma Grassy Bay Formation, Shaler Supergroup, Canada (Loron et al., 2019a), extending its biostratigraphic range to at least the entire Mesoproterozoic and probably into the early Neoproterozoic.

Moczydłowska et al. (2011) and Agić et al. (2015) suggested that *D. macoreticulata* could have been a cyst, opening through an operculate pylome excystment structure, as previously observed by Yin et al. (2005). The specimen bearing a circular pylome reported here (Fig. 4.7) supports this suggestion, although no operculum is evidenced. The presence of this elaborate structure and the tessellated nature of the wall of *D. macroreticulata* indicate that it was unambiguously a member of the total group eukaryote.

Dictyosphaera smaugi new species
Figure 5

Holotype.—Specimen 76091-R37, sample HB07-41A 183m; illustrated in Figure 5.1.

Diagnosis.—Spheroidal to subspheroidal vesicles with wall partly consisting of hexagonal platelets on less than one-third of the surface (most commonly one-sixth of the surface). The area made of platelets is irregular in shape and may vary in form and size, as well as number of plates (two dozen and more), from one specimen to another.

Occurrence.—Samples CL17-14, CL17-15, and HB07-41A 183 m, shale of the Fort Confidence Formation, Dismal Lakes Group, in the Dismal Lakes area, Nunavut, Canada.

Description.—Vesicles are 55.0 to 270.0 µm in diameter (average = 112.4 µm, n = 25). Platelet sizes are 1.5–2.5 µm.

Etymology.—From the J.R.R. Tolkien legendarium, "Smaug, the Golden" dragon, covered by an impenetrable scaled armor, save for his underbelly, in reference to the incompleteness of the platelet pattern on the microfossil vesicle surface.

Materials.—Fifty specimens recovered from samples CL17-14, CL17-15, and HB07-41A 183 m.

Remarks.—The surface ornamentation is consistent over the 50 specimens reported from the three different strata. This partial cover of platelets is not observed in any other microfossils from these samples. Therefore, it is unlikely that this ornamentation results from superimposition of different materials. The cover is consistently less than a third of the surface in each specimen reported for each stratum. Such consistency is unlikely to result from diagenetic processes as it would have implied that the degradations have stopped at the same stage and time for all specimens of the three samples.

D. smaugi differs from *D. macroreticulata* by its wall surface. In *D. macroreticulata*, the whole vesicle wall is made of small tessellated platelets, whereas in *D. smaugi* the wall is smooth except on one-third to one-sixth of its surface, where it consists of small polygonal tessellated platelets.

The complex microscale wall ornamentation of *D. smaugi* indicates an affinity of these microfossils to the total group eukaryote (Javaux et al., 2003).

Genus *Gangasphaera* (Prasad and Asher, 2001), emend.

Type species.—*Gangasphaera bulbousus* Prasad and Asher, 2001 (p. 70).

Emended diagnosis.—Vesicles spheroidal to subspheroidal bearing one or several prominent spheroidal or subspheroidal bulbous protrusions or extensions of the vesicle wall. The protrusions are rounded and closed at the distal end and freely communicate with the main vesicle.

Remarks.—The genus *Gangasphaera* was erected by Prasad and Asher (2001) to accommodate spheroidal to subspheroidal vesicles bearing one or two bulbous protrusions. The wall surface texture characterized by Prasad and Asher (2001, p. 70) as "chagrinate to microgranulate" and the described "irregular wrinkles or folds" probably resulted from taphonomy and should not be included in the genus diagnosis. The amended diagnosis used here accommodates specimens from other locations bearing more than two bulbous protrusions (see the following).

Gangasphaera bulbousus (Prasad and Asher, 2001), emend.
Figure 6.10–6.12

1989 Своеобразная форма с тремя пленчатымн придатками [peculiar form with three membranous appendages]; Jankauskas et al., p. 168, pl. 42, fig. 1.
1990 Densely packed cells widely ranging in size; Hermann, p. 18, pl. 4, fig. 10.
1990 Cell under gemmation; Hermann, p. 20, pl. 5, fig. 11.
1991 *Coneosphaera inaequalalis* Luo, p. 189, pl. 1, figs 1–3, 7.
non1991 *Coneosphaera inaequalalis* Luo, p. 189, pl. 1, figs 4–6.
1994 *Coneosphaera* sp.; Hofmann and Jackson, p. 30, fig. 18.14, 18.15.
1999 *Trachysphaeridium* cf. *T. laufeldi*; Yin and Guan, p. 135, fig. 5.1, 5.8, 5.10.
2001 *Gangasphaera bulbousus* Prasad and Asher, p. 69, pl. 11, figs. 1–5.

https://doi.org/10.1017/jpa.2021.45 Published online by Cambridge University Press

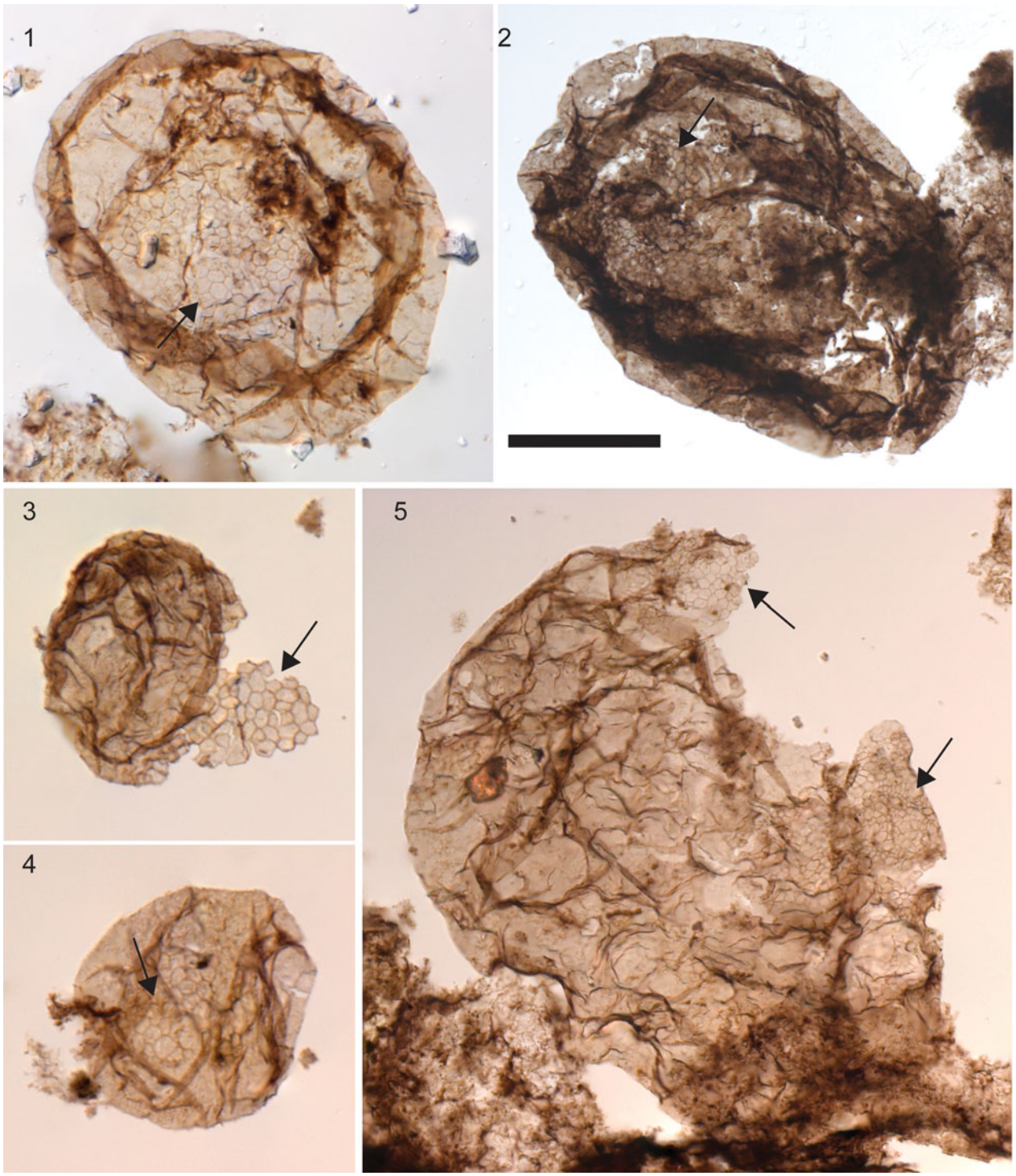

Figure 5. *Dictyosphaera smaugi* n. sp. with a mostly smooth wall but a restricted area made of polygonal platelets (arrows). (**1**) Holotype, 76091-r37. (**2**) 76085-o27. (**3**) 76514-m44. (**4**) 76514-j34,2. (**5**) 76520-p53. All photomicrographs taken under transmitted, plane-polarized light. (**1, 3–5**) are from sample HB07-41A 183 m; (**2**) is from sample CL17-14. Scale bar in (**2**) = 20 μm for (**1, 4**), 30 μm for (**3**), and 45 μm for (**2, 5**).

2016 *Coneosphaera* sp.; Baludikay et al., p. 170, fig. 8M, N.
2019a *Coneosphaera* sp.; Loron et al., p. 353, fig. 2S.
2017 *Coneosphaera* cf. *C.* sp.; Beghin et al., p. 68, pl. 1I.
2019 Sphaeromorphs likely in various stages of cell division; Li et al., p. 270, fig. 7I-7R.
non2019 Sphaeromorphs likely in various stages of cell division; Li et al., p. 270, fig. 7S, 7T.

Holotype.—Specimen UJN-D-A, DC-13 in Prasad and Asher (2001, pl. 11, fig. 1).

https://doi.org/10.1017/jpa.2021.45 Published online by Cambridge University Press

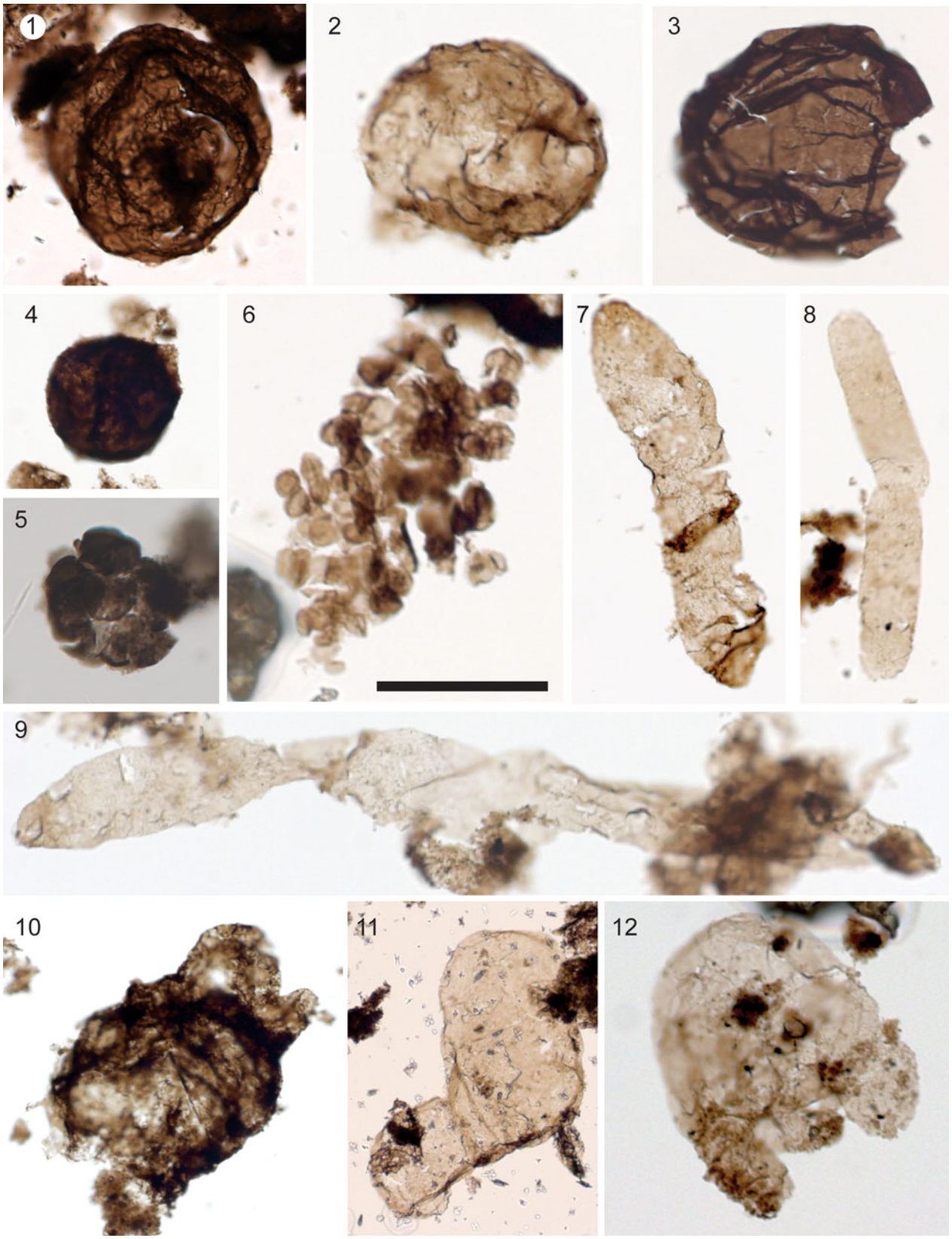

Figure 6. (**1–3**) *Leiosphaeridia* spp., nonornamented spheroidal vesicles: (**1**) *L. tenuissima*, 76090-w40; (**2**) *L. minutissima*, 76548-k53-2; (**3**) *L. tenuissima*, 76088-p32. (**4**) Leiosphere, unidentified spheroidal vesicle, 76092-w45. (**5**) *Synsphaeridium* sp., 75377-j48. (**6**) *Symplassiosphaeridium* sp., 76092-q40,2. (**7–9**) *Navifusa majensis*: (**7**) 76520-e41,2; (**8**) 76514-e56,3; (**9**) 76803-s28,2. (**10–12**) *Gangasphaera bulbousus*: (**10**) 76511-s36; (**11**) 76506-v28; (**12**) 76801-j34. All images taken under transmitted, plane-polarized light. (**1, 4, 6–12**) are from sample HB07-41A 183 m; (**2**) is from sample HB07-41A 232 m; (**3**) is from sample CL17-15; (**5**) is from sample 08RAT-K106. Scale bar in (**6**) = 30 μm for (**2, 5, 6**), 50 μm for (**1, 3, 4, 7, 8, 12**), 100 μm for (**9, 10**), and 150 μm for (**11**).

https://doi.org/10.1017/jpa.2021.45 Published online by Cambridge University Press

Emended diagnosis.—Spheroidal to subspheroidal vesicles bearing one to several spheroidal to subspheroidal bulbous protrusions. Protrusions are rounded at distal end and communicate freely with the vesicle interior.

Occurrences.—This form-taxa is ubiquitous and long ranging, spanning from the early Mesoproterozoic (Prasad and Asher, 2001; this study) to the Tonian (Jankauskas et al., 1989; Hermann, 1990; Li et al., 2019).

Description.—The vesicles are 43.1–103.9 µm in minimum diameter (n = 7). Bulbous protrusions are 8.4–82.5 µm in diameter (n = 10).

Material.—Eight specimens in sample HB07-41A 183 m.

Remarks.—The genus *Gangasphaera* was created by Prasad and Asher (2001) to accommodate spheroidal to subspheroidal specimens bearing one or two bulbous protrusions. They differ from the specimens reported as *Coneosphaera* sp. by Hofmann and Jackson (1994), Baludikay et al. (2016), Beghin et al. (2017), and Loron et al. (2019a) only in the number of protrusions. The original diagnosis of the genus *Coneosphaera* by Luo (1991) referred to "aggregated colonies of small spheroids surrounding a single, larger spheroid" (Luo, 1991, p. 189; Hofmann and Jackson, 1994, p. 30), which is not compatible with specimens from the aforementioned authors. These specimens fit the diagnosis of the genus *Gangasphaera* (Prasad and Asher, 2001), and so they are synonymized under its type species, *G. bulbousus* (Prasad and Asher, 2001) emend.

The original diagnosis of *G. bulbousus* (Prasad and Asher, 2001) included both size and taphonomic information. The wall surface texture characterized by Prasad and Asher (2001, p. 70) as "chagrinate to microgranulate" and the report of "irregular wrinkles or folds" are irrelevant for taxonomic diagnosis because they almost certainly result from taphonomy.

The large range of morphology and size documented in these microfossils does not exclude possible polyphyletism. In addition, the morphology of *G. bulbousus*, although certainly complex in its variability, does not show any strong, undeniably eukaryotic trait (Javaux et al., 2003) and cannot confidently be designated as either prokaryote or eukaryote (incertae sedis).

Genus *Germinosphaera* Mikhailova (1986) Butterfield in Butterfield et al., 1994

Type species.—*Germinosphaera bispinosa* Mikhailova, 1986, p. 33.

Remarks.—The genus *Germinosphaera* was created to accommodate process-bearing spheroidal vesicles with one or two tubular processes that communicate freely with the vesicle interior and are distributed on a single "equatorial" plane. On the basis of the number of processes, two distinct species were originally erected by Mikhailova (1986): *G. unispinosa* and *G. bispinosa*. Butterfield et al. (1994) reported specimens with a highly variable number of processes (one to six processes) and showed that the variable number of processes was intraspecific. The genus was emended, and the two species were subsumed into one type species, *G. bispinosa*.

In 2019, Miao and colleagues erected *G. alveolata*, a distinct species of *Germinosphaera*, on the basis of differences in the wall surface structure. The species is emended in the following to include the results of new SEM evidence.

The presence of processes, and surface ornamentation for *G. alveolata*, indicates that *Germinosphaera* is unambiguously eukaryotic (Javaux et al., 2003; Butterfield, 2015a). Although long, filamentous branching protrusions have recently been discovered on one new archaeon species (Imachi et al., 2020), and have been known in Planctomycetes–Verrucomicrobia–Chlamydiae (PVC) bacteria, showing that prokaryotes may show complex morphologies supported by their cytoskeleton, the size of *Germinosphaera,* and of many other Proterozoic organic-walled acanthomorphic microfossils, strongly differs by several orders of magnitude from this 0.5 µm archaeon and few-microns-sized bacteria. Moreover, these prokaryotes are unknown so far in the fossil record.

Germinosphaera alveolata (Miao et al., 2019), emend.
Figure 7.4–7.10

2019 *Germinosphaera alveolata* (Miao et al., 2019, p. 187, fig. 5g–k).

Holotype.—Specimen PB22506, ChL-CQ0501, Q/36 in Miao et al. (2019, fig. 5g).

Emended diagnosis.—"Spheroidal to slightly elongate vesicle with a single robust process extending gradually from the vesicle wall. Process is hollow, having a broad base, slightly tapering towards the end, and communicating freely with the vesicle cavity" (Miao et al., 2019, p. 187). Vesicle and process surface are ornamented with irregularly overlapping scale-like structures.

Occurrence.—Late Paleoproterozoic Chuanlinggou Formation, Changchang Group, China (Miao et al., 2019) and Mesoproterozoic Fort Confidence Formation, Dismal Lakes Group, Canada (this study).

Description.—Vesicles are 25.9–57.0 µm in diameter (n = 20). Processes are 5.0–14.3 µm wide (n = 20). The length of the processes is difficult to evaluate due to preservation (breakage). Scales are <1 µm in size.

Materials.—Materials include 144 specimens from sample HB07-41A 183 m.

Remarks.—This species constitutes an example of the limitations of optical microscopy in taxonomy. The "alveolar" surface pattern described by Miao et al. (2019) in the type specimens is similar in optical microscopy to the surface pattern of the present specimens from the Dismal Lakes Group, and the microfossils undoubtedly belong to the same species, but only electron microscopy revealed that this pattern

https://doi.org/10.1017/jpa.2021.45 Published online by Cambridge University Press

actually corresponds to overlapping organic scales forming the surface structures (Fig. 7.9, 7.10). For such complex taxa, electron microscopy constitutes a useful taxonomic tool.

Germinosphaera bispinosa (Mikhailova, 1986) Butterfield in Butterfield et al., 1994
Figure 4.4, 4.5

1986 *Germinosphaera bispinosa* Mikhailova, p. 33, fig. 6.
1986 *Germinosphaera unispinosa* Mikhailova, p. 33, fig. 5.
1994 *Germinosphaera bispinosa*; Butterfield in Butterfield et al., p. 38, fig. 16D, E.
2018 *Germinosphaera bispinosa*; Loron and Moczydłowska, p. 24, pl. 1, fig. 3.
2019a *Germinosphaera bispinosa*; Loron et al., p. 364, fig. 8E, F.

See Loron and Moczydłowska (2018) for extended synonymy.

Holotype.—Specimen no. 882/2 in Mikhailova (1986, fig. 6).

Occurrence.—Neoproterozoic (upper Riphean) Dashka Formation, East Siberian Platform, Siberia (Mikhailova, 1986); Neoproterozoic Svanbergfjellet Formation, Akademikerbreen Group Spitsbergen (Butterfield et al., 1994); Neoproterozoic upper formation, Visingsö Group, Sweden (Loron and Moczydłowska, 2018); late Mesoproterozoic Escape Rapids Formation and early Neoproterozoic Grassy Bay Formation, Shaler Supergroup, Canada (Loron et al., 2019a); Mesoproterozoic of the Fort Confidence Formation, Dismal Lakes Group, Canada (this study); and various other occurrences from the early Mesoproterozoic to early Cambrian (see Loron and Moczydłowska, 2018).

Description.—Smooth spheroidal vesicle (16.0–25.8 µm in diameter; n = 3) bearing one or two unbranched processes (10.5–12 µm in width; n = 4) that communicate freely with the vesicle interior.

Materials.—Three specimens from sample HB07-41A 183 m.

Remarks.—Butterfield et al. (1994) emended the species to include specimens with one to four processes, distributed on the equatorial plan of the vesicle, and synonymized *G. bispinosa* and *G. unispinosa* into *G. bispinosa* (according to name priority).

Genus *Lineaforma* Vorob'eva et al., 2015

Type species.—*Lineaforma elongata* Vorob'eva et al., 2015.

Lineaforma elongata Vorob'eva et al., 2015
Figure 7.1

2004 Large striated tubes, Javaux et al., p. 126, fig 3g–k.
2015 *Lineaforma elongata* Vorob'eva et al., p. 216, fig. 7.1–7.5.
2017 *Lineamorpha elongata*; Javaux and Knoll, p. 13, fig. 5.1–5.4.
2017 *Lineaforma elongata*; Adam et al., p. 388, fig. 2G, I.

Holotype.—Specimen GINPC 14711-804 in Vorob'eva et al. (2015, fig. 7.4).

Occurrence.—Early Mesoproterozoic Jalboi, Crawford, and Mainoru formations, Roper Group, Australia (Javaux et al., 2004; Javaux and Knoll, 2017); Fort Confidence Formation, Dismal Lakes Group, Canada (this study); Belt Supergroup, Montana (Adam et al., 2017); and Mesoproterozoic Kotuikan Formation, Siberia (Vorob'eva et al., 2015).

Description.—Longitudinally striated filament, 18.0–73.9 µm wide (n = 6). No complete filaments are found.

Materials.—Six fragmental specimens in samples CL17-14, HB07-41A 183m, and HB07-41A 232m.

Remarks.—Morphological and ultrastructural analyses (optical microscopy, SEM, transmission electron microscopy) of *L. elongata* specimens from the Roper Group, Australia, have shown that the striated surface sculpture of these large hollow filamentous tubes reflects original compositional heterogeneities in the tube wall, indicating complex physiological controls on wall formation different from bundles of filaments or fibrous wall ultrastructure known in prokaryotes (Javaux et al., 2004). The combination of an ornamented wall and a complex ultrastructure supports a eukaryotic interpretation for *L. elongata* tubes (Javaux et al., 2003, 2004; Javaux and Knoll, 2017).

Genus *Osculosphaera* (Butterfield in Butterfield et al., 1994) emend.

Type species.—*Osculosphaera hyalina* Butterfield in Butterfield et al., 1994.

Original diagnosis.—Psilate, hyaline spheroidal vesicles with a single, rimmed, circular opening, 25–50% the diameter of the vesicle (Butterfield et al., 1994, p. 43)

Emended diagnosis.—Smooth-walled vesicles with a single, circular opening. This opening might be operculate or not, and the operculum might be smooth-walled or ornamented.

Remarks.—Butterfield et al. (1994) erected this genus to accommodate spheroidal microfossils preserved in chert and bearing a rimmed circular opening. The circular opening of *Osculosphaera* is interpreted as a pylome, a regular circular excystment aperture that opens to liberate the cyst content. In microfossils, such openings might be operculate (e.g., *L. kulgunica* (Jankauskas et al., 1989) in Loron et al., 2019a, fig. 6E, F), operculate with an ornamented operculum (e.g., *Kaibabia gemmulella* Porter and Riedman, 2016 (fig. 7.1–7.9)), or not operculate (e.g., *L. kulgunica* in Jankauskas et al., 1989, pl. 11, figs. 8–10; *O. hyalina* in Butterfield et al., 1994, fig. 15F–J). The absence of an operculum might be due to preservation (detached and lost opercula) or original absence (formation of a pylome by enzymatic digestion of the wall). In the latter cases, it is possible that such a morphospecies actually includes several different biological entities.

https://doi.org/10.1017/jpa.2021.45 Published online by Cambridge University Press

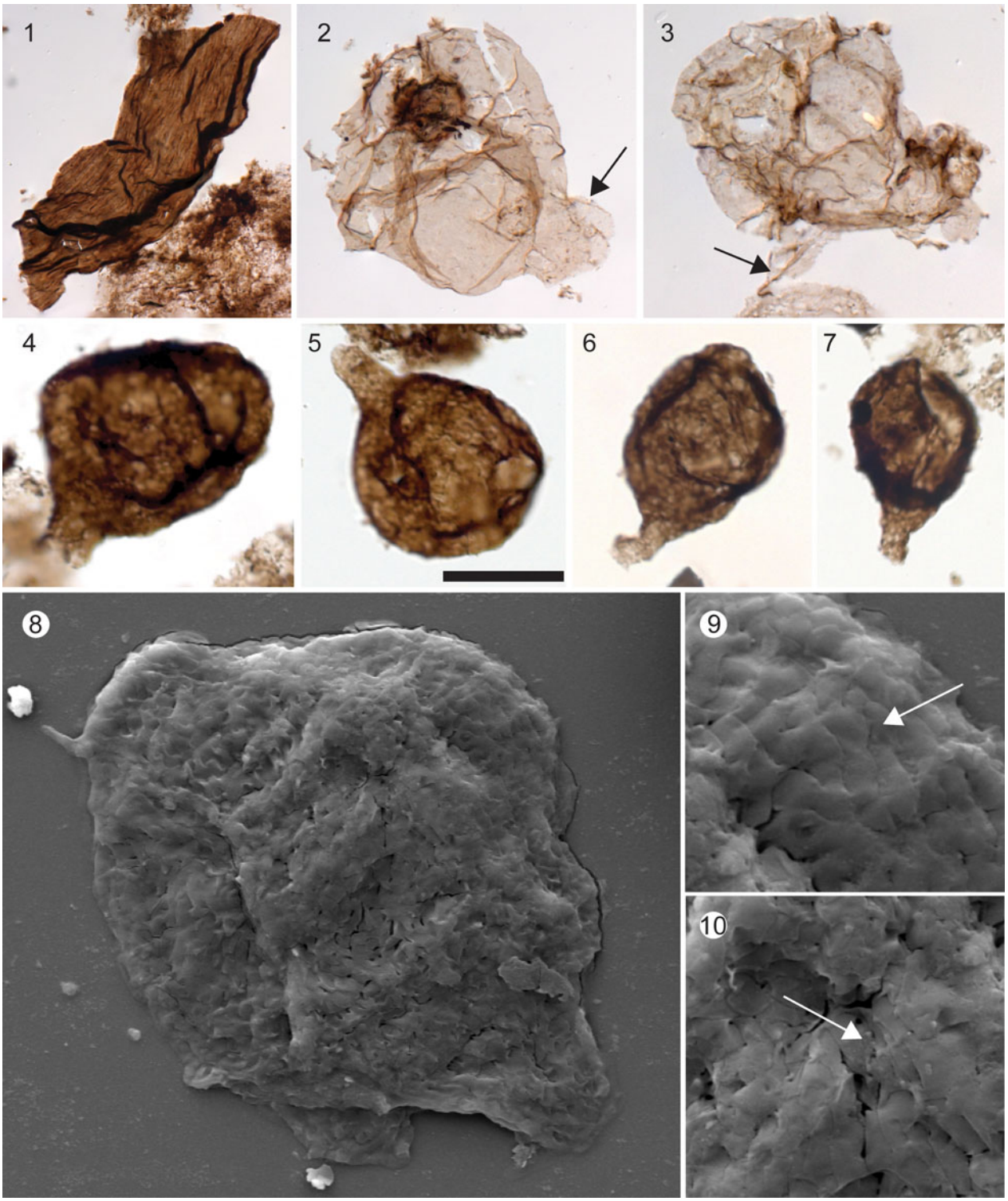

Figure 7. (**1**) *Lineaforma elongata*, 76517-f28. (**2, 3**) *Tappania*? sp.: (**2**) 76553-o30; (**3**) 76515-o58. (**4–10**) *Germinosphaera alveolata* emend.: (**4**) 76091-n29,3; (**5**) 76522-r59; (**6**) 76804-n37; (**7**) 76092-h45, 3; (**8–10**) DLFC-25; SEMs show the wall structure of the microfossils, made of overlapping polygonal scale-like plates (arrows in (**9**) and (**10**)). (**1–7**) Taken under a plane-polarized, transmitted light; (**1, 3–10**) are from sample HB07-41A 183 m; (**2**) is from sample HB07-41A 232 m. Scale bar in (**5**) = 2 μm for (**9, 10**), 5 μm for (**8**), 20 μm for (**4–7**), and 30 μm for (**1–3**).

Cell wall rupture to liberate the cell content can be observed in some pleurocapsalean cyanobacteria (Waterbury and Stanier, 1978), but the morphological complexity of a pylome (operculate or not) and required genetic and cellular machinery are unknown in prokaryotes (Javaux et al., 2003) and indicate a eukaryotic affinity.

Smooth-walled pylome-bearing forms are not rare in the Precambrian, and the presence of a circular excystment opening

https://doi.org/10.1017/jpa.2021.45 Published online by Cambridge University Press

constitutes the only substantial morphological distinction from specimens of the genus *Leiosphaeridia*. Some leiospheres were certainly precursors of these pylome-bearing microfossils (Butterfield et al., 1994). However, the presence of a pylome (a eukaryotic trait; Javaux et al., 2003) constitutes a criterion to erect a distinct genus from *Leiosphaeridia*, a basket genus gathering arbitrarily sorted smooth-walled spheroidal microfossils of uncertain biological affinity.

Following Butterfield et al. (1994), we propose here to recombine all smooth-walled pylome-bearing microfossils under the genus *Osculosphaera* and recognize three distinct morphospecies: (1) *O. gemmulella* (Porter and Riedman, 2016) n. comb., bearing an operculate pylome ornamented with numerous ~1 µm granulae; (2) *O. kulgunica* (Jankauskas et al., 1980) Butterfield et al., 1994, bearing a smooth-walled operculate pylome (operculum can be absent); and (3) *O. hyalina* Butterfield et al., 1994, bearing a non-operculate, rimmed, circular opening. In *O. kulgunica*, opercula were suggested lost by Jankauskas et al. (1989) and were detected only in microfossils reported by Loron et al. (2019a).

Loron and Moczydłowska (2018) erected the new species *L. gorda* on the basis of a smooth-walled specimen bearing a large, polygonal-shaped pylome opening. Only two specimens are illustrated, and one of them (pl. 2, fig. 4) might be modern contamination. They might constitute a distinct species of *Osculosphaera*, but this will require the observation of more convincing specimens.

A circular, sometimes operculated, excystment structure (pylome) requires the presence of a complex cytoskeleton, sophisticated genetic programming, and enzymatic machinery to digest and open the recalcitrant wall along a predetermined circular line and, thereby, constitutes an unambiguous character at the level of eukaryotic cellular complexity (Javaux et al., 2003, 2004; Javaux, 2007, 2011; Porter, 2020). Polyphyly remains possible within these form species, but it is now constrained within the domain eukaryote.

Osculosphaera hyalina Butterfield in Butterfield et al., 1994
Figure 4.6

1994 *Osculosphaera hyalina* Butterfield in Butterfield et al., p. 43, fig. 15F–J.

Holotype.—Specimen HUPC 627 1 6, illustrated by Butterfield et al. (1994, fig. I SF).

Occurrence.—Mesoproterozoic of the Fort Confidence Formation, Dismal Lakes Group, Canada (this study); Neoproterozoic of the Svanbergfjellet Formation, Spitsbergen (Butterfield et al., 1994).

Description.—Smooth-wall spheroidal vesicle ranging from 16.0 to 55.0 µm in minimum diameter (n = 5) and bearing a circular opening 6.7–19.5 µm in diameter (n = 5).

Materials.—Five specimens in samples CL17-14 and HB07-41A 183m.

Remarks.—Specimens of *Osculosphaera hyalina* reported by Nagovitsin (2009, fig. 5d, e) do not display a rimmed opening as diagnostic of the species and are, here, recognized as *O. kulgunica*.

Genus *Pterospermopsimorpha* (Timofeev, 1966) Mikhailova in Jankauskas et al., 1989

Type species.—*Pterospermopsimorpha pileiformis* Timofeev, 1966, emend. Mikhailova in Jankauskas et al., 1989.

Remarks.—The genus was described as morphotaxa corresponding to a vesicle enclosing another vesicle (disphaeromorph), with a smooth wall (*P. insolita* [Timofeev, 1969]) or granular wall (*P. pileiformis*). Sixteen different taxa were described for this genus (Fensome et al., 1990; Jachowicz-Zdanowska, 2013), but some of them were subsequently synonymized and subsumed in *P. insolita* (see Loron and Moczydłowska, 2018). Opening of the outer vesicle through medial split is observed in some specimens (e.g., Loron et al., 2019a, fig. 8C).

The morphology of *Pterospermopsimorpha* is similar to the phycoma (resting stage) of prasinophyte algae, and affinity to this clade of eukaryote has been proposed by several authors (e.g., Tappan, 1980; Inouye et al., 1990; Guy-Ohlsson, 1996; Samuelsson et al., 1999; Moczydłowska et al., 2011; Moczydłowska, 2016). However, the possibility of morphological convergence cannot be discarded, and without further information about their ultrastructure and wall chemistry, specimens of *Pterospermopsimorpha* cannot be interpreted as unambiguous crown-group eukaryotes. The presence of a recalcitrant vesicle within another recalcitrant vesicle has been suggested to indicate the presence of cytoskeleton and organelles (Parke et al., 1978; Graham and Wilcox, 2000), unknown in prokaryotes. Regardless of taxonomy, we interpret *Pterospermopsimorpha* as a member of the total group eukaryote because of the combination of a disphaeromorph morphology and the presence of granular ornamentation on the external vesicle and of medial split openings in some specimens. The combination of these characters differs from bacterial colonial envelopes enclosing several small cells.

Pterospermopsimorpha insolita (Timofeev, 1969) Mikhailova in Jankauskas et al., 1989
Figure 4.3

1969 *Pterospermopsimorpha insolita* Timofeev, p. 16, pl. 3, fig. 8.
1989 *Pterospermopsimorpha insolita*; Mikhailova in Jankauskas et al., 1989.
2016 *Pterospermopsimorpha insolita*; Riedman and Porter, p. 873, fig. 12.6–12.9.
2016 *Pterospermopsimorpha insolita*; Baludikay et al., p. 170, fig. 7I–L.
2017 *Pterospermopsimorpha insolita*; Beghin et al., p. 73, pl. 3., figs. b–d.
2017 *Pterospermopsimorpha insolita*; Agić et al., p. 113, fig. 10A–C.
2018 *Pterospermopsimorpha insolita*; Loron and Moczydłowska, p. 18, pl. 4, figs. 1–6.

https://doi.org/10.1017/jpa.2021.45 Published online by Cambridge University Press

2019a *Pterospermopsimorpha insolita*; Loron et al., p. 358, fig. 8B, C.
2019 *Pterospermopsimorpha insolita*; Miao et al., p. 189, fig. 7a–d.

For extended synonymy see Loron and Moczydłowska (2018) and Miao et al. (2019).

Holotype.—Specimen with preparation number 16/5 illustrated by Timofeev (1969, p. 16, pl. 3, fig. 8). Jankauskas et al. (1989) reported the holotype as lost. Lectotype was selected from the same location and illustrated: preparation number 16/42 in Jankauskas et al. (1989, p. 49, pl. 3, fig. 6).

Occurrence.—This long-ranging taxon is cosmopolitan in the Precambrian. It has been reported worldwide from the late Paleoproterozoic (Agić et al., 2017; Miao et al., 2019) to mid-Neoproterozoic (Riedman and Porter, 2016).

Description.—Smooth-walled spheroidal vesicle enclosing another, more opaque, vesicle. The outer vesicle is 55.5–292.5 µm in minimum diameter, and the inner vesicle is 35.0–116.5 µm in minimum diameter (n = 5).

Materials.—Five specimens reported from samples HB07-41A 183m and HB07-41A 232m.

Remarks.—It is possible that *P. insolita* represents a developmental variant of *Leiospheria* spp. that are simple smooth-walled vesicles and could correspond to the empty outer vesicle for *P. insolita* or to its inner vesicle without the external envelope.

Genus *Satka* (Jankauskas, 1979) Loron et al., 2019a

Type species.—*Sakta favosa* (Jankauskas, 1979).

Remarks.—The genus *Satka* was originally divided into six species (Jankauskas et al., 1989). *Satka elongata* Jankauskas et al., 1989 and *S. granulosa* Jankauskas et al., 1989 were synonymized with *S. favosa* by Javaux and Knoll (2017), and *Satka colonialica* Jankauskas, 1979 was combined with the genus *Squamosphaera* (Tang et al., 2015). Loron et al. (2019a) followed the reevaluation of Tang et al. (2015) and emendation by Porter and Riedman (2016) and recognized *Squamosphaera* as a distinct genus from *Satka*. Loron et al. (2019a) proposed to remove *Satka undosa* Jankauskas, 1979 from the genus and to recombine it with *Synsphaeridium*. Similarly, they recombined *Satka squamosphaera* Pyatiletov, 1980 with the genus *Squamosphaera*. The genus *Satka* originally included lobate forms (now *Squamosphaera*) and forms made of polygonal plates (*Satka favosa*). For this reason, it was emended to conform with the description of its type species: *Satka favosa* (Loron et al., 2019a).

Sakta favosa Jankauskas, 1979
Figure 4.10, 4.11

1979 *Satka favosa* Jankauskas, pl. 4, fig. 2.
1989 *Satka favosa*; Jankauskas et al., p. 51, pl. 4, figs. 1, 2?
1989 *Satka elongata*; Jankauskas et al., p. 51, pl. 4, figs. 3, 5.
1989 *Satka granulosa*; Jankauskas et al., p. 51, pl. 4, fig. 8.
1989 *Satka squamifera*; Jankauskas et al., p. 51, pl. 5, figs. 3, 8.
1994 *Satka* spp.; Hofmann and Jackson, pl. 18, figs. 26–31.
2017 *Satka favosa*; Javaux and Knoll, p. 15, figs. 5.6–5.9.
2019a *Sakta favosa*; Loron et al., p. 371, fig. 7A–D.

See Loron et al. (2019a) for extended synonymy and discussion.

Holotype.—Specimen with preparation number 16–1815-635 in Jankauskas et al. (1989, pl. 4, fig. 2).

Occurrence.—Mesoproterozoic Fort Confidence Formation, Dismal Lakes Group, Canada (this study); Greyson Formation, Belt Supergoup, Montana (Adam et al., 2017); Eqalulik Formation, Bylot Supergroup, Canada (Hofmann and Jackson, 1994); Mainoru Formation, Roper Group, Australia (Javaux and Knoll, 2017); Kamov, Chuktukon, Terina and Brus formations of the southern Urals (Jankauskas et al., 1989); and late Mesoproterozoic–early Neoproterozoic Grassy Bay and Nelson formations, Shaler Supergroup, Canada (Loron et al., 2019a).

Description.—Hollow spheroidal vesicles, ranging from 27.6 to 41.2 µm in minimal diameter (n = 5), with a wall made of tessellated polygonal plates. The plates are 3.7–7.0 µm in size (n = 13).

Materials.—Seventeen specimens from samples CL17-07, HB07-41A 183m, and 08RAT-K106.

Remarks.—The wall of *S. favosa*, made of tessellated organic plates, implies the presence of a complex cellular machinery that is indicative of its eukaryotic nature (Javaux et al., 2003). By comparison, the simpler bulging envelopes of *Squamosphaera* could be prokaryotic in origin. The original genus *Satka* was, before reassignment by Loron et al. (2019a), most probably gathering polyphyletic biological species belonging to either domain (Eukaryota and Bacteria). Within the form species *Satka favosa*, although polyphyletism remains possible, it is constrained within eukaryotes.

Genus *Simia* Mikhailova and Jankauskas in Jankauskas et al., 1989

Type species.—*Simia simica* (Jankauskas, 1980) Jankauskas, 1989.

Simia annulare (Timofeev, 1969) Mikhailova in Jankauskas et al., 1989
Figure 4.2

1969 *Pterospermopsimorpha annulare* Timofeev, p. 17, pl. 3, fig. 9.
2009 *Ostiumsphaeridium complitum*; Vorob'eva et al., p. 186, fig. 14.1–14.5.
2013 *Simia annulare*; Tang et al., p. 162, fig. 4G.

https://doi.org/10.1017/jpa.2021.45 Published online by Cambridge University Press

2016 *Simia annulare*; Riedman and Porter, p. 874, fig. 12.1–12.5.
2017 *Simia annulare*; Agić et al., p. 118, figs. 10FI, 14H, I.
2017 *Simia annulare*; Beghin et al., p. 73, pl. 3, fig. e.
2018 *Simia annulare*; Loron and Moczydłowska, p. 21, pl. 5, figs. 1–3.
2019 *Simia annulare*; Miao et al., p. 192, fig. 7e–g.
2019a *Simia annulare*; Loron et al., p. 358, fig. 8A.

Holotype.—Specimen with preparation number 147/4 illustrated by Timofeev (1969, pl. 3, fig. 9).

Occurrence.—This long-ranging fossil is present from the late Paleoproterozoic–early Mesoproterozoic (Miao et al., 2019) to the Ediacaran (Vorob'eva et al., 2009).

Description.—Spheroidal vesicles bearing an equatorial flange. The vesicle diameter is ranging from 62.5 to 105.5 µm and the flange is 5–7.5 µm wide (n = 7).

Materials.—Nineteen specimens recovered from the samples HB07-41A 183m, HB07-41A 232m, and 08RAT-K106.

Remarks.—As mentioned by Riedman and Porter (2016), there was much confusion between the pteromorph (vesicle bearing an equatorial flange) genus *Simia* and the disphaeromorph (vesicle enclosing another vesicle) genus *Pterospermopsimorpha*. Because of the equatorial development of its flange, *Simia* resembles the genus *Pterospermella* known in the Phanerozoic successions since the Cambrian (Eisenack, 1972; Moczydłowska, 2016) and reported from the Neoproterozoic (Loron and Moczydłowska, 2018), but *Pterospermella* is a disphaeromorph and not a pteromorph (see discussion in Loron and Moczydłowska, 2018).

Many authors have interpreted vesicles of *Simia* (along with *Pterospermopsimorpha* and *Pterospermella*) as members of the class Prasynophyceae (e.g., Tappan, 1980; Inouye et al., 1990; Playford, 2003; Moczydłowska et al., 2011; Moczydłowska, 2016). The large equatorial flange ornamenting the vesicles of *Simia annulare* is a complex morphology that ascribes them with confidence among eukaryotes (Javaux et al., 2003). However, despite morphological resemblance with modern prasinophytes (e.g., *Pterosperma*), further ultrastructural and chemical analyses are required to identify *Simia* as a stem or crown eukaryote.

Genus *Spiromorpha* Yin et al., 2005

Type species.—*Spiromorpha segmentata* (Prasad and Asher, 2001) Yin et al., 2005.

Spiromorpha segmentata (Prasad and Asher, 2001) Yin et al., 2005
Figure 4.12–4.14

2001 *Navifusa segmentatus* Prasad and Asher, p. 77, pl. 5, figs. 4, 5, 14, 15.
2005 *Spiromorpha segmentata*; Yin et al., p. 57, fig. 5.1, 5.4–5.8.
2009 "short trichomes containing terminal lenticular and medial arcuate cells"; Nagovitsin, p. 143, fig. 5h, i.
2015 *Spiromorpha* sp.; Pang et al., p. 254, fig. 2C.
2017 *Spiromorpha segmentata*; Beghin et al., p. 73, pl. 3, figs. o, p.

Holotype.—Specimen KDM-A, 5204-07m, originally *Navifusa segmentatus* (Prasad and Asher, 2001, pl. 5, fig. 5).

Occurrence.—Late Paleoproterozoic–early Mesoproterozoic Beidajian Formation, Ruyang Group, China (Yin et al., 2005; Pang et al., 2015); Mesoproterozoic (early middle Riphean) Sarda and Avadh formations, Bahraich Group, India (Prasad and Asher, 2001); Mesoproterozoic of the Fort Confidence Formation, Dismal Lakes Group, Canada (this study); Mesoproterozoic Yurubchen and Dzhelindukon formations, Kamo Group, Siberia (Nagovitsin, 2009); and late Mesoproterozoic Khatt Formation, Atar/El Mreïti Group, Mauritania (Beghin et al., 2017).

Description.—Smooth-walled oval-shaped vesicle, 40.0–114.5 µm long and 15.0–38.5 µm wide (n = 13). Grooves are spirally distributed from one extremity of the vesicle to the other, each groove is ≤1 µm wide.

Materials.—Thirty-nine specimens reported from sample HB07-41A 183m.

Remarks.—The grooves present on the vesicle surface of *S. segmentata* are not septae but a surface sculpture (Beghin et al., 2017). Here we agree and recognize *S. segmentata* as a total group eukaryote on the basis of the presence of this microscale surface ornamentation (Javaux et al., 2003).

The morphology, with spiral grooves, of *S. segmentata* closely resembles the basal algal taxon *Spirotaenia* (Yin et al., 2005). Further investigations of their ultrastructure and chemistry might unravel a crown-group affinity to these microfossils.

Genus *Tappania* Yin, 1997

Type species.—*Tappania plana* Yin, 1997.

Tappania? sp.
Figure 7.2, 7.3

2016 ?cf. *Tappania sp.* Baludikay et al., p. 173, figs. 6R, 7A, B.

Description.—Spheroidal to subspheroidal smooth-walled vesicles bearing trapezoidal protrusions and neck-like extensions. One possible process is present on one specimen (Fig. 7.3).

Materials.—Six specimens from samples CL17-15, HB07-41A 183m, and HB07-41A 232m.

Remarks.—The present specimens resemble specimens of *Tappania plana* with neck-like extensions but lack the

https://doi.org/10.1017/jpa.2021.45 Published online by Cambridge University Press

diagnostic tubular processes of the species (see Javaux and Knoll, 2017, fig. 6.5, 6.6). In our material, one specimen (Fig. 7.3) bears what might be a process, but it is possible that this results from taphonomic superimposition. In the absence of all diagnostic characters of the species, we cannot unambiguously recognize these microfossils as *Tappania plana*.

In *Tappania*? sp. the neck-like extensions are trapezoidal, differing from the bulbous spheroidal protrusion of *Gangasphaera bulbousus*.

The complex morphology of *Tappania* indicates the presence of a dynamic cytoskeleton and endomembrane system, which allow their unambiguous placement within eukaryotes (see discussion in Javaux et al., 2001; Javaux and Knoll, 2017). In the absence of taxonomic certainty, we cautiously recognize our specimens of *Tappania*? sp. as probable eukaryotes. Examination of more specimens of this material is necessary to confirm their identification.

Genus *Valeria* Jankauskas, 1982

Type species.—*Valeria lophostriata* (Jankauskas, 1979) Jankauskas, 1982.

Valeria lophostriata (Jankauskas, 1979) Jankauskas, 1982
Figure 4.1

1979 *Kildinella lophostriata* Jankauskas, p. 153, fig. 1.13–1.15.
1982 *Valeria lophostriata*; Jankauskas, p. 109, pl. 39, fig. 2.
1989 *Valeria lophostriata*; Jankauskas et al., p. 86, pl. 16, figs. 1–5.
2004 *Valeria lophostriata*; Javaux et al., fig. 2F–I.
2009 *Valeria lophostriata*; Nagy et al., fig. 1A, B.
2015 *Valeria lophostriata*; Tang et al., p. 315, fig. 11.
2016 *Valeria lophostriata*; Riedman and Porter, p. 10, fig. 4.1.
2016 *Valeria lophostriata*; Porter and Riedman, fig. 19.1–19.3.
2016 *Valeria lophostriata*; Baludikay et al., p. 170, fig. 7H.
2017 *Valeria lophostriata*; Beghin et al., p. 73, pl. 4, fig. j, k.
2017 *Valeria lophostriata*; Agić et al., p. 119, fig. 12I.
2019a *Valeria lophostriata*; Loron et al., p. 356, fig. 4E.
2019 *Valeria lophostriata*; Miao et al., p. 194, fig. 11a–f.

Holotype.—Specimen number 16-62-4762/16, sp. 1 illustrated by Jankauskas (1979, fig. 1.14).

Occurrence.—This long-ranging taxon is found worldwide throughout the Proterozoic, from the late Paleoproterozoic (Javaux et al., 2004; Agić et al., 2017; Miao et al., 2019) to the Cryogenian (Nagy et al., 2009).

Description.—Large spheroidal vesicle (35.0–205.0 µm minimum diameter; n = 13) bearing conspicuous surface ornamentation made of concentric ridges ("archery target" pattern). Medial split opening of some vesicles is observed.

Materials.—Materials include 111 specimens reported from samples CL17-15, HB07-41A 183m, HB07-41A 232m, and 08RAT-K106.

Remarks.—The distinctive micron-scale regularly spaced concentric striations on the inner surface of the recalcitrant wall of *Valeria,* combined with the common occurrence of medial split excystment structure, indicate its eukaryotic affinity as such combination is unknown in prokaryotes (Javaux et al., 2003, 2004). Butterfield (2015a) pointed out the similarity of this surface pattern with the one observed on the wall of the cyanobacteria *Glaucocystis*, formed by cellulose fibrils. However, in *Glaucocystis,* the fibrils are at the nanoscale (~10 nm wide), are cross-linked, and constitute the ultrastructure of the cell wall rather than an ornamentation (Willison and Brown, 1978).

Unnamed sp. A
Figure 8.8

Description.—Filamentous microfossil, 21.4 µm wide and 209 µm long, with one flattened and thickened extremity. The opposite extremity is separated into three lobes with rounded shapes.

Material.—One single filament in sample CL17-14.

Remarks.—Such a complex morphology would allow the placement of this specimen among eukaryotes but needs to be confirmed by examination of more specimens to discard possible taphonomic artefact; therefore, it is left in open nomenclature.

Shale-hosted microfossils of the Dismal Lakes Group

Previous investigations of the Dismal Lakes Group biota reported a very low diversity of organic-walled microfossils. A study of chert samples from the Kendall River, Dease Lake, and Greenhorn River formations yielded a low diversity of prokaryotic filamentous and coccoidal microfossils (Horodyski and Donaldson, 1980, 1983). Thin sections of shale from the lower Greenhorn Formation revealed spheroidal and filamentous microfossils of *Leiospheridia* and *Siphonophycus* genera (Horodyski et al., 1980). In previous reports, no fossils with eukaryotic attributes were described. Our reinvestigation of this historical material (thin sections GSC-64157, GSC-64158, and GSC-67159) yielded identical conclusions (Figs. 3, 9).

The present work describes 24 different taxa, one new species, and one unnamed form recovered from shales of the middle Dease Lake and Fort Confidence formations, strata that were not investigated for paleontology by Horodyski and Donaldson (1980, 1983).

Filamentous forms.—Filamentous forms are present in all of the fossiliferous samples with the exception of the sample from the Dease Lake Formation. Nonseptate empty sheaths of *Siphonophycus* (Schopf, 1968) Knoll, Swett, and Mark, 1991 are the most abundant (Fig. 8.1, 8.2) and may be assigned to seven of the size-class species described by Butterfield et al. (1994) and Tang et al. (2015): *Siphonophycus septatum* (Schopf, 1968) Knoll, Swett, and Mark, 1991 (1.0–2.0 µm wide); *S. robustum* (Schopf, 1968) Knoll, Swett, and Mark,

https://doi.org/10.1017/jpa.2021.45 Published online by Cambridge University Press

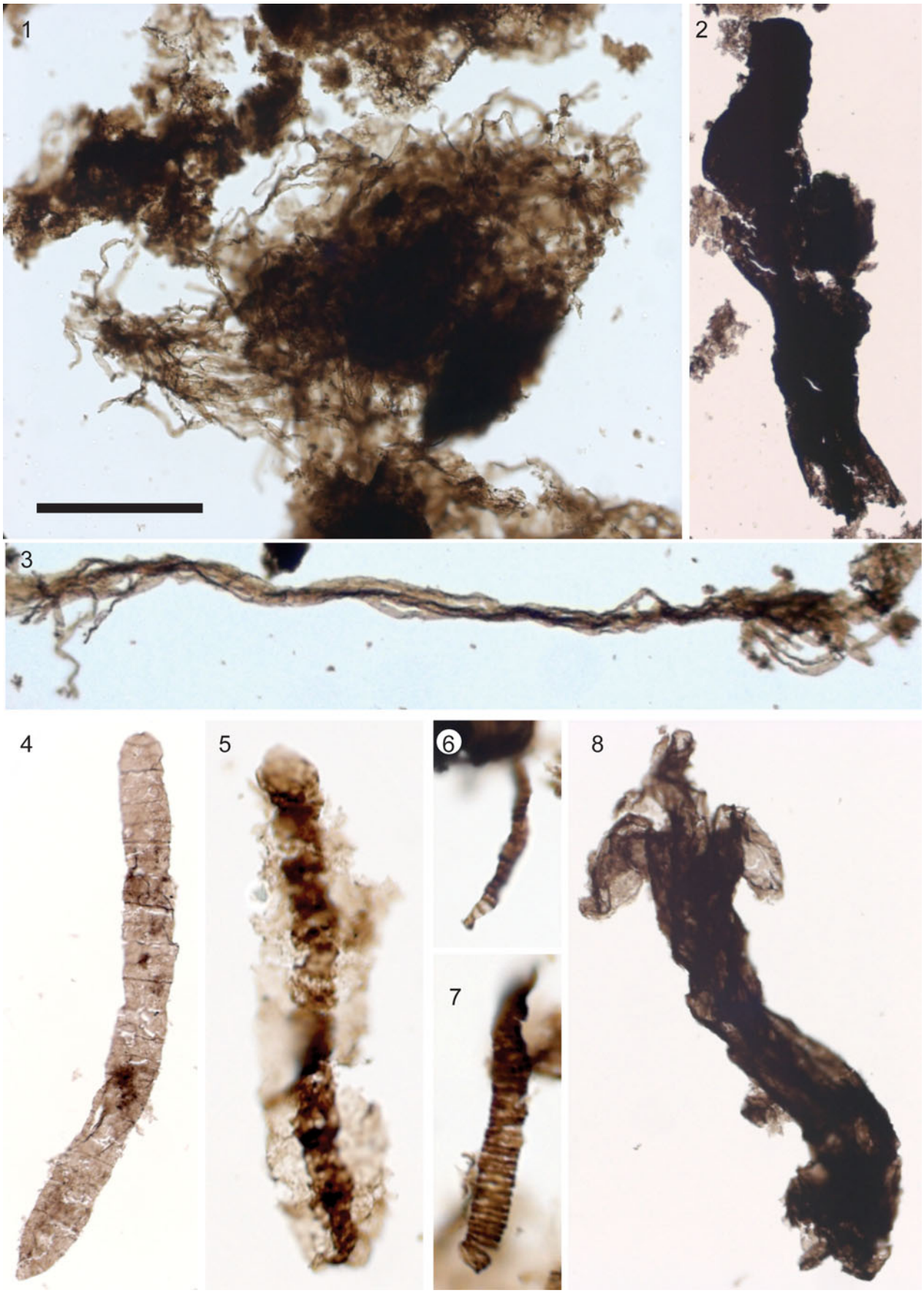

https://doi.org/10.1017/jpa.2021.45 Published online by Cambridge University Press

Figure 8. Filamentous forms. (**1**) Mat of *Siphonophyccus* spp., 76553-u49. (**2**) *Syphonophyccus gigas*, 76085-l46. (**3**) *Polythrichoides lineatus*. (**4**) *Oscillatoriopsis* sp., 76085-e53,3. (**5**) *Palaeolyngbya* sp., 76092-n44,4. (**6**) *Tortunema* sp., 76802-p31-1. (**7**) *Cephalonyx* sp., 76804-j36. (**8**) Unnamed species A with trilobate extremity, 76084-p41. All photomicrographs taken under transmitted, plane-polarized light. (**1**) is from sample HB07-41A 232 m; (**2, 3, 8**) are from sample CL17-14; (**5–7**) are from sample HB07-41A 183 m. Scale bar in (**1**) = 30 µm for (**5–7**), 60 µm for (**1, 4**), 120 µm for (**3, 8**), and 200 µm for (**2**).

1991 (2.1–4.0 µm wide); *S. typicum* (Hermann, 1974) Butterfield in Butterfield et al., 1994 (4.1–8.0 µm wide); *S. kestron* Schopf, 1968 (8.1–16.0 µm wide); *S. solidum* (Golub, 1979) Butterfield in Butterfield et al., 1994 (16.1–32.0 µm wide); *S. punctatum* Maithy, 1975 (32.1–64.0 µm wide); and *S. gigas* Tang et al., 2015 (64.1–128.0 µm wide). Bundles of tightly packed parallel filamentous sheaths are present and identified as *Polytrichoides lineatus* (Hermann, 1974) (Fig. 8.3). Uniseriate trichomes of *Oscillatoriopsis* (Schopf, 1968) Butterfield in Butterfield et al., 1994 and pseudoseptate filaments of *Tortunema* (Hermann, 1974) Butterfield in Butterfield et al., 1994 are also present (Fig. 8.4, 8.6) as well as a single specimen of *Palaeolyngbya* (Schopf, 1968) Butterfield in Butterfield et al., 1994, with the sheath enclosing remains of the original cells (Fig. 8.5). A small filament with regularly distributed annular bulges is recognized as *Cephalonyx* Weiss, 1984 (5.5 µm wide, n = 1; Fig. 8.7), and a large unknown form with a trilobate extremity is reported (unnamed species A; Fig. 8.8).

Unornamented microfossils.—Spheroidal unornamented vesicles of *Leiosphaerida* spp. constitute the main abundance of the assemblage (Fig. 6.1–6.3). In this assemblage, the arbitrary size-class species of *Leiosphaeridia crassa* (Naumova, 1949) Jankauskas et al., 1989: *L. minutissima* (Naumova, 1949) Jankauskas in Jankauskas et al., 1989*;* *L. jacutica* (Timofeev, 1966) Jankauskas in Jankauskas et al., 1989*;* and *L. tenuissima* Eisenack, 1958 can be recognized on the basis of the size of the vesicles (<70 µm for *L. minutissima* and *L. crassa*; >70µm for *L. jacutica* and *L. tenuissima*) and shape of the folds indicating wall flexibility (sinuous for *L. minutissima* and *L. tenuissima*; lanceolate for *L. crassa* and *L. jacutica*) following the principles of Javaux and Knoll (2017). However, a large number of specimens in different samples are opaque and do not display conspicuous taphonomic folds or cracks (leiospheres; Fig. 6.4). These size-class species are morphotaxa that are probably polyphyletic and do not necessarily coincide with biological species, but they are a useful tool to describe diversity of forms within an assemblage and to compare with previous micropaleontological studies.

Aggregates of smooth vesicles are also common in the assemblages, including clusters of closely attached (*Synsphaeridium* spp.; Fig. 6.5) and loosely attached (*Symplassiosphaeridium* spp.; Fig. 6.6) vesicles.

Elongated vesicles of *Navifusa majensis* Pyatiletov, 1980 (25.0–246.8 µm long and 2.5–40.0 µm wide; n = 12) are common (Fig. 6.7–6.9). In sample HB07-41A 183m (Fort Confidence Formation), many of the small specimens of this species (Fig. 6.8) are very similar to ovoidal specimens of *Archeoellipsoides* preserved in chert (Horodyski and Donaldson, 1980, 1983) and may, possibly, constitute their shale-hosted equivalent.

In addition, spheroidal and subspheroidal vesicles with one or several bulbous protrusions are recognized as *Gangasphaera bulbousus*, a form species with a large morphological variability (Fig. 6.10–6.12).

Ornamented microfossils.—The long-ranging taxon *Valeria lophostriata*, with characteristic circular ridges on the wall inner surface, is abundant throughout the assemblage (Fig. 4.1). Rare specimens of *Simia annulare* ornamented with an equatorial flange and the disphaeromorph (vesicle

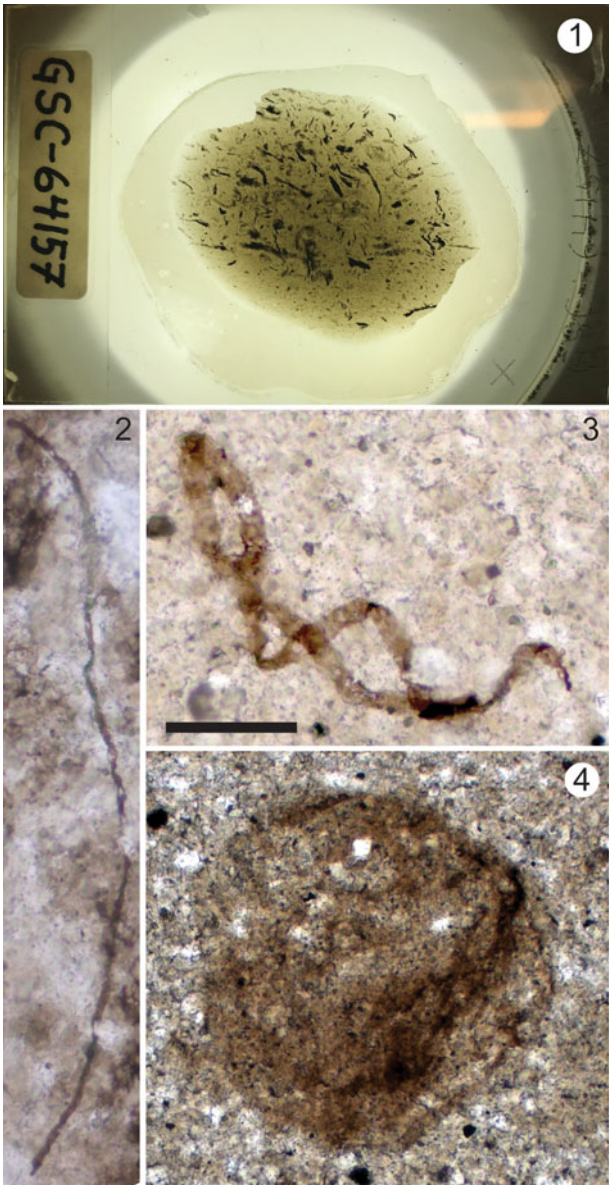

Figure 9. New images of historical material from Horodyski at al. (1980). (**1**) Photomicrograph of shale in thin-section GSC-64157; note the abundance of organic material (black). (**2, 3**) *Siphonophycus* spp. (**4**) *Leiosphaeridia* sp. All images are of thin-sectioned (thick section) shale taken under transmitted, plane-polarized light; (**2–4**) are from thin-section GSC-64159. Scale bar in (**3**) = 1,500 µm for (**1**), 150 µm for (**3**), and 50 µm for (**2, 4**).

https://doi.org/10.1017/jpa.2021.45 Published online by Cambridge University Press

enclosing another vesicle) *Pterospermopsimorpha insolita* are also recognized (Fig. 4.2, 4.3). In addition, five specimens of *Osculosphaera hyalina*, with a pylome excystment structure (circular opening) are documented (Fig. 4.6). Vesicles of *Dictyosphaera macroreticulata* (Fig. 4.7–4.9) and *Satka favosa* (Fig. 4.10, 4.11) are also present. *D. macroreticulata* has a wall made of tessellate hexagonal plates, whereas wall plates of *S. favosa* are larger, fewer, and have a polygonal or quadrate shape (see Javaux and Knoll, 2017 and Loron et al., 2019a for discussion of this species). Oval vesicles ornamented with spiral grooves, *S. segmentata* (Fig. 4.12–4.14), are abundant, and rare fragments of *Lineaforma elongata*, a large tube with longitudinal striations on its wall surface, also occur. We also report the presence of a new taxa, *Dictyosphaera smaugi* n. sp. (Fig. 5). These microfossils possess a smooth wall except for a localized area of their wall made of hexagonal platelets (see Fig. 5.1–5.5). As opposed to *D. macroreticulata*, these structures do not form the whole vesicle wall but are present only on one irregularly shaped area representing less than one-third of the vesicle wall surface.

Acanthomorphic (processes-bearing) microfossils.—Three specimens of *Germinosphaera bispinosa* are present, one of them bearing two equatorial processes (Fig. 4.4, 4.5). The Fort Confidence assemblage also includes the second report of *Germinosphaera alveolata* (Fig. 7.4–7.10). SEM reveals that the microfossils are covered with small overlapping scale-like structures (Fig. 7.8–7.10) and not alveoli as suggested in its original description (Miao et al., 2019).

Six specimens of *Tappania*? sp. were recovered from samples CL17-15, HB07-41A 183 m, and HB07-41A 232 m (32.0–65.3 µm in size; n = 6); these microfossils are irregularly shaped and have neck-like expansions. One specimen might bear a process (Fig. 7.2, 7.3).

Discussion

The moderate diversity of organic-walled microfossils recovered from the shale units of the Dismal Lakes Group, especially from the Fort Confidence Formation, provide new insights on early Mesoproterozoic life. The 24 described taxa most certainly include members of both eukaryotic and prokaryotic domains.

Affinity of Dismal Lakes Group microfossils.—Several authors have proposed criteria to recognize eukaryotic fossils within assemblages. The presence of surface ornamentation, complex wall ultrastructure, complex excystment structure (e.g., a pylome, or circular opening, with occasionally an operculum preserved, to release the cell content), as well as the presence of processes, complex multicellularity, and eukaryotic biopolymers making up the wall, constitute characteristics unknown in prokaryotes (Javaux et al., 2001, 2003, 2004; Javaux and Marshall, 2006; Knoll et al., 2006). As discussed, although long filamentous branching protrusions have recently been discovered on one new archaeon species (Imachi et al., 2020) and verrucae and processes are known in some PVC bacteria, showing that prokaryotes may show complex morphologies supported by their cytoskeleton, the size of the vesicle and ornamentation of Proterozoic organic-walled acanthomorphic microfossils strongly differ by several orders of magnitude from these smaller-than-a-micron- to a-few-microns-sized prokaryotes. Moreover, these prokaryotes are not known to form kerogenous walls fossilized in the geological record. These examples illustrate why most of the criteria listed in the preceding need to be used in combination to discriminate eukaryotic from prokaryotic microfossils.

Similarly, Butterfield (2015a) suggests that conspicuous surface ornamentations, processes, and "true" multicellularity (with specialized cells) may unambiguously classify a microfossil as eukaryotic but went further by suggesting that they would indicate a placement among crown eukaryotes. The size of the microfossils, although informative when combined with other criteria, is not valid on its own since the existence of giant bacteria and micro-eukaryote is now well established (Javaux et al., 2003). Among the 24 taxa reported from the assemblage, we interpret 11 of them as being unambiguously eukaryotic because they have one particularly complex character or combine several of these characters (see Table 1).

The characters observed on the ornamented fossils *V. lophostriata*, *S. annulare*, *P. insolita*, *O. hyalina*, *D. smaugi* n. sp., *D. macroreticulata*, *S. favosa*, *S. segmentata*, *L. elongata*, and process-bearing *G. bispinosa* and *G. alvaeolata* indicate the evolution of various biological innovations, showing a eukaryotic grade of cellular complexity such as the presence of a complex cytoskeleton and possibly an endomembrane system (Javaux et al., 2003, 2006; Javaux and Marshall, 2006; Butterfield, 2015a). According to criteria from Butterfield (2015a), some of the most complex ornamented and process-bearing forms reported here (*Dictyosphaera, Satka favosa, Germinosphaera alveolata*) might even represent crown eukaryotes. However, without further complementary investigations of their wall ultrastructure and chemistry, and in the absence of taxonomically diagnostic characters, their stem or crown nature cannot be confirmed unambiguously. Nevertheless, the degree of morphological complexity achieved by the reported specimens indicates that the lineages represented by these microfossils have radiated after the first eukaryotic common ancestor (FECA), and although it is unknown whether they belong to stem (before LECA) or crown (after LECA) groups, they are members of the total group eukaryotes and, therefore, no longer considered prokaryotic.

By comparison, specimens of *Leiosphaeridia* spp., *Navifusa majensis*, *Gangasphaera bulbousus*, and the colonial forms *Synsphaeridium* spp. and *Symplassiosphaeridium* spp. cannot unequivocally be interpreted as eukaryotes as they do not preserve any diagnostic eukaryotic morphological characters. Careful multi-proxy studies of *Leiospharidia* wall ultrastructure and composition in the Proterozoic and in the Cambrian have shown that some of them were probably eukaryotic in origin (e.g., Arouri et al., 2000; Talyzina and Moczydłowska, 2000; Javaux et al., 2004; Moczydłowska and Willman, 2009), but such analyses have not yet been conducted on the Dismal Lakes microfossils. These few examples illustrate a possible hidden diversity within leiospheres but cannot be extrapolated to all leiospheres through the geological record without further extensive investigations.

In addition, because of the simple but still variable morphology and size distribution of these microfossils, it is possible

https://doi.org/10.1017/jpa.2021.45 Published online by Cambridge University Press

Table 1. Microfossil features characteristic of eukaryotic affinity.

Microfossil	Processes	Surface ornamentation	Tessellated wall	Pylome	Vesicle enclosing another vesicle
Dictyosphaera macroreticulata			X	X	
Dictyosphaera smaugi n. sp.			X		
Germinosphaera alveolata	X	X			
Germinosphaera bispinosa	X				
Lineaforma elongata		X			
Osculosphaera hyalina				X	
Pterospermospimorpha insolita					X
Satka favosa			X		
Simia anulare		X			
Spiromorpha segmentata		X			
Valeria lophostriata		X			

that they were polyphyletic or that the specimens recovered represent developmental variants of the same biological entity. Unnamed sp. A might present a complex morphology, but this needs to be confirmed to discard possible taphonomic artefact since only a single specimen was observed. The possible eukaryotic affinity of *Tappania*? sp. remains ambiguous as they display only the neck-like extension diagnostic of this species but no unequivocal processes. More specimens need to be discovered to correctly assign them to the species *Tappania plana* and the eukaryotic domain.

The remaining simple filamentous forms are globally too simple in their morphology to be recognized as eukaryotic and are usually interpreted as remains of mat-building cyanobacteria (Butterfield et al., 1994; Demoulin et al., 2019).

Biostratigraphic significance of Dismal Lake Group acritarchs.—The shale-hosted biota of the Dismal Lakes Group is typical of Proterozoic assemblages, containing abundant sphaeromorphs and filaments. In addition, this assemblage contains diverse ornamented and processes-bearing taxa, identified as eukaryotes (at least 11) and is comparable in diversity only to the biota of the Ruyang Group in China for the late Paleoproterozoic–early Mesoproterozoic period. Most of these eukaryotes are widespread in Proterozoic assemblages worldwide (*Valeria, Pterospermopsimorpha*) or characteristic of Mesoproterozoic assemblages (*Lineaforma, Satka favosa, Dictyosphaera macroreticulata*; but see Loron et al., 2019a for younger occurrences of *S. favosa* and *D. macroreticulata*). One species is new (*D. smaugi*), and finally, this is the second occurrence of *Germinosphaera alveolata*, and the first in the early Mesoproterozoic, as it was previously reported only from shales of the late Paleoproterozoic Changzhougou Formation, China (Miao et al., 2019). The Dismal assemblage also contains one of the oldest known specimens of *O. hyalina*, a pylome-bearing microfossil previously reported only from the Neoproterozoic (Butterfield et al., 1994). In addition, the pylome excystment structure documented here on *Dictyosphaera macroreticulata* (Fig. 4.7) confirms the suggestion that this species opened in a more complex way than simple medial splitting (Yin et al., 2005; Moczydłowska et al., 2011; Agić et al., 2015).

The high diversity of eukaryotes in the Dismal Lakes assemblage is unusual for early Mesoproterozoic strata. Other contemporaneous successions of shale-hosted microfossils record no more than six eukaryotic taxa—Bahraich Group (Prasad and Asher, 2001); Billyakh Group (Vorob'eva et al., 2015); Roper Group (Javaux and Knoll, 2017); Belt Supergroup (Adam et al., 2017); Changcheng Group (Miao et al., 2019); lower Vindhyan Supergroup (Prasad et al., 2005)—with the exception of the Ruyang Group (Yin et al., 2005; Agić et al., 2015, 2017) and the Kamo Group (Nagovitsin, 2009) (Table 2). The assemblages from China, Australia, Laurentia (USA and Canada), and India generally contain the same taxa, whereas Siberian assemblages are more distinct but similar to assemblages described from younger successions, with the exception of *Spiromorpha segmentata* and *Tappania plana* in the Kamo Group (Nagovitsin, 2009) and *Lineaforma* in the Billyakh Group (Vorob'eva et al., 2015). The presence of common taxa indicates that independent oceanic basins were connected. Conversely, the paleogeographic distance of the Siberian localities from the other documented successions might explain their differences, along with facies variations (although all are from shallow-water marine successions). The Siberian successions are, however, poorly dated and may be younger than early Mesoproterozoic. In addition, favorable taphonomic conditions have inevitably played a role in the apparent diversity of fossils in the China, Australia, and Laurentia successions, and sampling bias must also be considered (Cohen and Macdonald, 2015).

Implication for early eukaryotic evolution.—LECA is thought to have possessed a complex system of endomembrane, a nucleus, a sophisticated cytoskeleton of actin and tubulin, and a complex cellular machinery typical of modern protists. It was capable of phagotrophy, meiosis, and aerobic metabolism and was probably heterotroph (see López-García and Moreira, 2015 for review; Koonin, 2010; Koumandou et al., 2013). In the fossil record, the silicified remains of *Bangiomorpha pubescens* Butterfield, 2000 from the 1047 +0.013/–0.017 Ga Hunting Formation, Canada (Butterfield, 2000; Gibson et al., 2017) were interpreted as multicellular red algae. Recently, large benthic multicellular organic remains of *Proterocladus antiquus* Tang et al., 2020 from the 1056 ± 22 to 947.8 ± 7.4 Ma Nanfen Formation, North China (Tang et al., 2020) were recognized as a member of the crown group Chlorophyta (green algae). Together, they provide a minimum age for LECA and for eukaryotic photosynthesis (a crown trait), implying an earlier evolution of unicellular algae and an older origin for a unicellular and nonphototroph LECA (Javaux, 2007). Older 1.6 Ga fossils, also interpreted as red algae (Bengtson et al., 2017), and molecular clocks (Parfrey et al., 2011; Eme et al., 2014) suggest an older minimum age for LECA, but the age and identity of the fossils are debated (Gibson et al., 2017; Betts

https://doi.org/10.1017/jpa.2021.45 Published online by Cambridge University Press

Table 2. Eukaryotic diversity of contemporaneous successions of late Paleoproterozoic–early Mesoproterozoic. In bold are taxa shared with the Dismal Lakes Group.

Beidajian and Baicaoping formations	Changzhougou and Chuanlinggou formations	Deonar, Koldaha, Salkhan, Rampur, Rohtasgarh and Bhagawar formations	Dease Lake and Fort Confidence formations	Greyson Formation
Ruyang Group	Changcheng Group	Semri Group, Vindhyan Supergroup	Dismal Lakes Group	Belt Supergroup
China	China	India	Canada	USA (Montana)
1744 ± 22 to 1411 ± 27 Ma	1673 ± 10 to 1638 ± 14 Ma	1630.7 ± 0.4 to 1599 ± 48 Ma	<1600 to 1438 ± 5 Ma	1576 ± 13 to 1454 ± 9 Ma
Agić et al. (2015, 2017)	Miao et al. (2019)	Prasad et al. (2005); Ray (2006)	This study	Adam et al. (2017)
Dictyosphaera macroreticulata	***Germinosphaera alveolata***	***Pterospermospimorpha insolita***	***Dictyosphaera macroreticulata***	***Lineaforma elongata***
Gigantosphaeridium fibratum Agić et al., 2015	***Dictyosphaera macroreticulata***	***Satka favosa***	***Dictyosphaera smaugi* n. sp.**	***Satka favosa***
Gigantosphaeridium floccosum Agić et al., 2017	***Germinosphaera bispinosa***	***Simia anulare***	***Germinosphaera alveolata***	*Tappania plana*
Pterospermospimorpha insolita	***Pterospermospimorpha insolita***	***Spiromorpha segmentata***	***Germinosphaera bispinosa***	
Pterospermospimorpha saccata Yin, 1987	***Simia anulare***	*Tappania plana*	***Lineaforma elongata***	
Shuiyousphaeridium macroreticulatum (Yin, 1997) Agić et al., 2015	***Valeria lophostriata***		***Osculosphaera hyalina***	
Shuiyousphaeridium pilatum Li in Li et al., 2012			***Pterospermospimorpha insolita***	
Shuiyousphaeridium sp.			***Satka favosa***	
Simia anulare			***Simia anulare***	
Spiromorpha segmentata			***Spiromorpha segmentata***	
Tappania plana			***Valeria lophostriata***	
"Trachyhystrichosphaera"				
Valeria lophostriata				
Vidalopalla granulata Vidal in Vidal and Siedlecka, 1983				
Lower Kotuikan Formation	Vedreshe, Yurubchen and Dzhelindukon formations	McMinn, Velkerri, Corcoran, Jalboi, Crawford and Mainoru formations	Avadh and Sarda formations	
Billyakh Group	Kamo Group	Roper Group	Bahraich Group	
Siberia	Siberia	Australia	India	
1513 ± 51 to 1459±10	1499 ± 43 to 1060 ± 20 Ma	1492 ± 4 to 1361 ± 21 Ma	ca. 1350–1150 Ma	
Vorob'eva et al. (2015)	Nagovitsin (2009)	Javaux and Knoll (2017)	Prasad and Asher (2001)	
Lineaforma elongata	*Lophosphaeridium* sp.	*Blastanosphaira kokkoda* Javaux and Knoll, 2017	***Germinosphaera bispinosa***	
Palaeastrum dyptocranum Butterfield in Butterfield et al., 1994	*Osculosphaera kulgunica*	***Dictyosphaera macroreticulata***	*Pterospermospimorpha pileiformis*	
Pterospermopsimorpha pileiformis	*Pulvinosphaeridium* sp.	***Lineaforma elongata***	***Simia anulare***	
	Satka sp.	***Satka favosa***	***Spiromorpha segmentata***	
	Spiromorpha segmentata	*Tappania plana*	*Tappania plana*	
	Tappania plana	***Valeria lophostriata***		
	Tasmanites sp.			
	Valeria elongata			
	Valeria lophostriata			

et al., 2018). An alternative view proposes that *Bangiomorpha* provides a maximum age for LECA (Porter, 2020).

Stem/crown groups' dynamic and molecular-clock estimates indicate that crown groups diverge in the 300 Ma following the appearance of a last common ancestor (Eme et al., 2014), or even faster (Budd and Mann, 2019). On the basis of these rates, an early appearance of LECA at the end of the Paleoproterozoic, followed by a very discreet presence of crown groups before the end of the Mesoproterozoic (as observed in the fossil record) seems to be inconsistent with these estimations. Conversely, a late LECA, in the late Mesoproterozoic, implies that eukaryotic microfossils reported before that time were all, in fact, stem eukaryotes, possessing some, but not all, crown eukaryote attributes (Porter, 2020). Porter (2020) suggested that the discrepancy between crown/stem mathematical models and the fossil/biomarker record supports the hypothesis of LECA emerging not before 1100 Ma (maximum age), with the crown group being fully installed by 800 Ma. An alternative hypothesis could be that crown groups are present already in the early fossil record but unrecognized before the late Mesoproterozoic. These early crown-group members may have remained undetected because of many biases and the incompleteness of the fossil and sampling record (Cohen and MacDonald, 2015), the taphonomic conditions, the lack of resolution and gap of knowledge in proxies, biology, and biomarkers despite potential, but debated, candidates for early multicellular crown-group eukaryotes in the early Mesoproterozoic, such as *Rafatazmia* and *Ramathallus* (Bengtson et al., 2017) and *Palaeoastrum diptocranum* (Vorob'eva et al., 2015; Butterfield, 2015b, who also points out that convergence is possible with other nonphotosynthetic protists). Moreover, fossils such as *Bangiomorpha, Proterocladus*, and the aforementioned potential earlier candidates are multicellular complex forms that certainly do not represent the basal taxa of any branches of the eukaryotic tree.

In the fossil record, complex excystment structures, along with vesicles bearing regularly distributed processes, are characteristic of Neoproterozoic and Paleozoic organic-walled microfossils (Butterfield, 1997). The presence of microfossils with evenly

https://doi.org/10.1017/jpa.2021.45 Published online by Cambridge University Press

distributed processes in late Paleoproterozoic–early Mesoproterozoic rock (*Shuiyousphaeridium* and *Gigantosphaeridium* in the Ruyang Group; Javaux et al., 2003; Yin et al., 2005; Agić et al., 2015, 2017), with complex excystment structures, such as *O. hyalina* and *D. macroreticulata* in the present work, or possibly *Tappania plana* in Javaux and Knoll (2017) and Prasad et al. (2005), indicates that by the early Mesoproterozoic, eukaryotes had already acquired the cellular complexity to develop such features. Moreover, sedimentology for the Fort Confidence Formation indicates deposition in a shallow tidal-influenced environment. The presence of infilled desiccation cracks in the samples suggests occasional aerial exposure (Rainbird et al., 2020). Although atmospheric and oceanic redox conditions were fluctuating temporally and spatially in the Mesoproterozoic, the report of eukaryotic microfossils from such a shallow photic environment suggests that some of these early protists may have lived in slightly oxygenated waters, may have resisted oxidative stress, and therefore may have already possessed mitochondria. However, this remains to be tested by paleoredox proxies and paleoecological analyses.

Together with their diversity, the degree of morphological complexity and the speculative possibility of aerobic metabolism suggest that these eukaryotes evolved shortly before or after LECA. However, only further analyses of their ultrastructure, chemistry, and ecology may provide arguments supporting this hypothesis. Therefore, the Dismal Lake Group assemblage may include both stem eukaryotes and stem or crown clades within the crown eukaryotic supergroups, as proposed for the contemporaneous Roper Group assemblage (Javaux and Knoll, 2017). It is plausible that this radiation was linked to particular environmental conditions and/or ecological interactions and biological innovations in the late Paleoproterozoic–early Mesoproterozoic, although paleoenvironmental data remain too sparse to establish a robust correlation. The hypothesis of an early crown radiation, coupled with biological innovations, was suggested by |Javaux (2007, 2011) as the second stage of a three-stage model of early eukaryotic evolution. Butterfield (2015a) and Parfrey et al. (2011) also suggested an older LECA. Agić et al. (2017) suggested an initial eukaryotic diversification in the Mesoproterozoic, linked to innovations in eukaryotic body plans, that set the stage for a second diversification event in the Tonian.

Conclusions

Previous studies of the ca. 1600–1430 Ma Dismal Lakes Group in the Canadian Arctic yielded simple microfossils but no eukaryotic forms. This new study builds on this earlier work with the first systematic investigation of shale-hosted fossils of the Dease Lake and Fort Confidence formations. The moderate diversity of 24 taxa includes 11 unambiguous eukaryotes that were not previously documented in these strata, including one new species (*Dictyosphaera smaugi*). This level of eukaryotic diversity is similar to that reported from slightly older successions in China and contributes to the growing understanding of eukaryotic diversity in the early Mesoproterozoic. The morphological complexity of the eukaryotic fossils (e.g., pylomes, processes, organic plates, ridges and scales) and their diversity in the Dismal Lakes Group (Canada), China, India, Australia, and USA collectively support the emerging view that eukaryotes first diversified in the late Paleoproterozoic to early Mesoproterozoic, shortly before, or possibly shortly after, LECA. Although this early diversification may have been associated with unique paleogeographic or paleoenvironmental conditions, the possible controls for the mechanisms driving early eukaryotic diversification remain to be rigorously investigated.

Acknowledgments

This research was supported by the Agouron Institute, the FRS-FNRS, the ERC Stg ELiTE FP7/308074, and the FRS-FNRS-FWO EOS ET-HOME. We gratefully thank M. Giraldo, A. Lambion (U. Liege), and S. Borensztajn (IPGP, France) for their technical support, the Geological Survey of Canada's Geomapping for Energy and Minerals Program for the fieldwork logistics, and B. Davis (Geological Survey of Canada, Ottawa), J. Mercadier (CNRS, France), and V. Cumming for assistance during sample collection.

Data availability statement

Data available from the Dryad Digital Repository: https://doi.org/10.5061/dryad.zpc866t8b.

References

Adam, Z.R., Skidmore, M.L., Mogk, D.W., and Butterfield, N.J., 2017, A Laurentian record of the earliest fossil eukaryotes: Geology, v. 45, p. 387–390.
Agić, H., Moczydłowska, M., and Yin, L.M., 2015, Affinity, life cycle, and intracellular complexity of organic-walled microfossils from the Mesoproterozoic of Shanxi, China: Journal of Paleontology, v. 89, p. 28–50.
Agić, H., Moczydłowska, M., and Yin, L., 2017, Diversity of organic-walled microfossils from the early Mesoproterozoic Ruyang Group, North China Craton—a window into the early eukaryote evolution: Precambrian Research, v. 297, p. 101–130.
Arouri, K., Greenwood, P.F., and Walter, M.R., 1999, A possible chlorophycean affinity of some Neoproterozoic acritarchs: Organic Geochemistry, v. 30, p. 1323–1337.
Arouri, K.R., Greenwood, P.F., and Walter, M.R., 2000, Biological affinities of Neoproterozoic acritarchs from Australia: microscopic and chemical characterization: Organic Geochemistry, v. 31, p. 75–89.
Baludikay, B.K., Storme, J.Y., François, C., Baudet, D., and Javaux, E.J., 2016, A diverse and exquisitely preserved organic-walled microfossil assemblage from the Meso-Neoproterozoic Mbuji-Mayi Supergroup (Democratic Republic of Congo) and implications for Proterozoic biostratigraphy: Precambrian Research, v. 281, p. 166–184.
Baragar, W.R.A., and Donaldson, J.A., 1973, Coppermine and Dismal lakes map-areas 86 O and 86 N: Geological Survey of Canada Paper 71-39, 20 p.
Bartley, J.K., Kah, L.C., Frank, T.D., and Lyons, T.W., 2015, Deep-water microbialites of the Mesoproterozoic Dismal Lakes Group: microbial growth, lithification, and implications for coniform stromatolites: Geobiology, v. 13 p. 15–32.
Beghin, J., Storme, J.Y., Blanpied, C., Gueneli, N., Brocks, J.J., Poulton, S.W., and Javaux, E.J., 2017, Microfossils from the late Mesoproterozoic–early Neoproterozoic Atar/El Mreïti Group, Taoudeni Basin, Mauritania, northwestern Africa: Precambrian Research, v. 291, p. 63–82.
Bengtson, S., Sallstedt, T., Belivanova, V., and Whitehouse, M., 2017, Three-dimensional preservation of cellular and subcellular structures suggests 1.6 billion-year-old crown-group red algae: PLOS Biology, v. 15, e2000735.
Berbee, M.L., Strullu-Derrien, C., Delaux, P.M., Strother, P.K., Kenrick, P., Selosse, M.A., and Taylor, J.W., 2020, Genomic and fossil windows into the secret lives of the most ancient fungi: Nature Reviews Microbiology, v. 18, p. 717–730.
Betts, H.C., Puttick, M.N., Clark, J.W., Williams, T.A., Donoghue, P.C., and Pisani, D., 2018, Integrated genomic and fossil evidence illuminates life's early evolution and eukaryote origin: Nature Ecology and Evolution, v. 2, p. 1556–1562.

https://doi.org/10.1017/jpa.2021.45 Published online by Cambridge University Press

Bonneville, S., Delpomdor, F., Préat, A., Chevalier, C., Araki, T., Kazemian, M., Steele, A., Schreiber, A., Wirth, R., and Benning, L.G., 2020, Molecular identification of fungi microfossils in a Neoproterozoic shale rock: Science Advances, v. 6, p.eaax7599.
Bosak, T., Macdonald, F., Lahr, D., and Matys, E., 2011a, Putative Cryogenian ciliates from Mongolia: Geology, v. 39, p. 1123–1126.
Bosak, T., Lahr, D.J.G., Pruss, S.B., Macdonald, F.A., Dalton, L., and Matys, E., 2011b, Agglutinated tests in post-Sturtian cap carbonates of Namibia and Mongolia: Earth and Planetary Science Letters, v. 308, p. 29–40.
Bosak, T., Lahr, D.J.G., Pruss, S.B., Macdonald, F.A., Gooday, A.J., Dalton, L., and Matys, E.D., 2012, Possible early foraminiferans in post-Sturtian (716–635 Ma) cap carbonates: Geology, v. 40, p. 67–70.
Brocks, J.J., Jarrett, A.J.M., Sirantoine, E., Hallmann, C., Hoshino, Y., and Liyanage, T., 2017, The rise of algae in Cryogenian oceans and the emergence of animals: Nature, v. 548, p. 578–581.
Budd, G.E., and Mann, R.P., 2019, The dynamics of stem and crown groups: Science Advances, v. 6, eaaz1626.
Butterfield, N.J., 1997, Plankton ecology and the Proterozoic–Phanerozoic transition: Paleobiology, v. 23, p. 247–262.
Butterfield, N.J., 2000, *Bangiomorpha pubescens*: Paleobiology, v. 26, p. 386–404.
Butterfield, N.J., 2004, A vaucheriacean alga from the middle Neoproterozoic of Spitsbergen: implications for the evolution of Proterozoic eukaryotes and the Cambrian Explosion: Paleobiology, v. 30, p. 231–252.
Butterfield, N.J., 2009, Modes of pre-Ediacaran multicellularity: Precambrian Research, v. 173, p. 201–211.
Butterfield, N.J., 2015a, Early evolution of the Eukaryota: Palaeontology, v. 58, p. 5–17.
Butterfield, N.J., 2015b, Proterozoic photosynthesis—a critical review: Palaeontology, v. 58, p. 953–972.
Butterfield, N.J., Knoll, A.H., and Swett, K., 1994, Paleobiology of the Neoproterozoic Svanbergfjellet Formation, Spitsbergen: Lethaia, v. 27, p. 76.
Bykova, N., LoDuca, S.T., Ye, Q., Marusin, V., Grazhdankin, D., and Xiao, S., 2020, Seaweeds through time: morphological and ecological analysis of Proterozoic and early Paleozoic benthic macroalgae: Precambrian Research, v. 350, p. 105875.
Cohen, P.A., and Macdonald, F.A., 2015, The Proterozoic record of eukaryotes: Paleobiology, v. 41, p. 610–632.
Cohen, P.A., and Riedman, L.A., 2018, It's a protist-eat-protist world: recalcitrance, predation, and evolution in the Tonian–Cryogenian ocean: Emerging Topics in Life Sciences, v. 2, p. 173–180.
Cohen, P.A., Vizcaíno, M., and Anderson, R.P., 2020, Oldest fossil ciliates from the Cryogenian glacial interlude reinterpreted as possible red algal spores: Palaeontology, v. 63, p. 941–950.
Cornet, Y., François, C., Compère, P., Callec, Y., Roberty, S., Plumier, J.C., and Javaux, E.J., 2019, New insights on the paleobiology, biostratigraphy and paleogeography of the pre-Sturtian microfossil index taxon Cerebrosphaera: Precambrian Research, v. 332, 105410.
Demoulin, C.F., Lara, Y.J., Cornet, L., François, C., Baurain, D., Wilmotte, A., and Javaux, E.J., 2019, Cyanobacteria evolution: insight from the fossil record: Free Radical Biology and Medecine, v. 140, p. 206–223.
Dong, L., and Xiao, S., 2006, On the morphological and ecological history of Proterozoic macroalgae, *in* Xiao, S., and Kaufman, A.J., eds., Neoproterozoic Geobiology and Paleobiology: Dordrecht, Springer, p. 57–90.
Eisenack, A., 1958, Tasmanites Newton 1975 und Leiosphaeridia n. gen. aus gattungen der Hystrichosphaeridea: Palaeontographica Abteilung A, v. 110, p. 1–19.
Eisenack, A., 1972, Kritische Bemerkung zur Gattung Pterospermopsis (Chlorophyta, Prasinophyceae): Neues Jahrbuch Geologie Paleaontologie, v. 10, p. 596–601.
Eme, L., Sharpe, S.C., Brown, M.W., and Roger, A.J., 2014, On the age of eukaryotes: evaluating evidence from fossils and molecular clocks: Cold Spring Harbor Perspectives in Biology, v. 6, a016139.
Fensome, R.A., Williams, G.L., Barss, M.S., Freeman, J.M., and Hill, J.M., 1990, Acritarchs and fossil prasinophytes: an index to genera, species and infraspecific taxa: American Association of Stratigraphic Palynologists Contributions Series, v. 25, 771 p.
Frank, T.D., Kah, L.C., and Lyons, T.W., 2003, Changes in organic matter production and accumulation as a mechanism for isotopic evolution in the Mesoproterozoic ocean: Geological Magazine, v. 140, p. 397–420.
French, J.E., Heaman, L.M., and Chacko, T., 2002, Feasibility of chemical U–Th–total Pb baddeleyite dating by electron microprobe: Chemical Geology, v. 188, p. 85–104.
Gibson, T.M., et al., 2017, Precise age of *Bangiomorpha pubescens* dates the origin of eukaryotic photosynthesis: Geology, v. 46, p. 135–138.
Golub, I.N., 1979, A new group of problematic microfossils from Vendian deposits of the Orshan depression (Russian Platform), *in* Sokolov, B.S., ed., Paleontology of Precambrian and Early Cambrian: Leningrad, Nauka, p. 147–155. [in Russian]
Graham, L.E., and Wilcox, L.W., 2000, Algae: Upper Saddle River, New Jersey, Prentice Hall, 640 p.
Grey, K., 1999, A modified palynological preparation technique for the extraction of large Neoproterozoic acanthomorph acritarchs and other acid-soluble microfossils: Geological Survey of Western Australia, Department of Mineral and Energy, record 1999/10.
Guy-Ohlson D., 1996, Prasinophycean algae, *in* Jansonius, J., and McGregor, D.C., eds., Palynology: Principles and Applications, v. 1: Salt Lake City, American Association of Stratigraphic Palynologists Foundation, p. 181–189.
Hamilton, M.A., and Buchan, K.L., 2010, U-Pb geochronology of the Western Channel Diabase, northwestern Laurentia: implications for a large 1.59 Ga magmatic province, Laurentia's APWP and paleocontinental reconstructions of Laurentia, Baltica and Gawler craton of southern Australia: Precambrian Research, v. 183, p. 463–473.
Hermann, T.N., 1974, Findings of mass accumulations of trichomes in the Riphean, *in* Timofeev, B.V., ed., Proterozoic and Paleozoic Microfossils of the USSR: Moscow, Nauka, p. 6–10. [in Russian]
Hermann, T.N., 1990, Organic World Billion Year Ago: Leningrad, Nauka.
Hofmann, H.J., and Jackson, G.D., 1994, Shale-facies microfossils from the Proterozoic Bylot Supergroup, Baffin Island, Canada: Journal of Paleontology, v. 68, p. 1–35.
Horodyski, R.J., and Donaldson, J.A., 1980, Microfossils from the middle Proterozoic Dismal Lakes groups, arctic Canada: Precambrian Research, v. 11, p. 125–159.
Horodyski, R.J., and Donaldson, J.A., 1983, Distribution and significance of microfossils in cherts of the middle Proterozoic Dismal Lakes Group, District of Mackenzie, Northwest Territories, Canada: Journal of Paleontology, v. 57, p. 271–288.
Horodyski, R.J., Donaldson, J.A., and Kerans, C., 1980, A new shale-facies microbiota from the middle Proterozoic Dismal Lakes Group, District of Mackenzie, Northwest Territories, Canada: Canadian Journal of Earth Sciences, v. 17, p. 1166–1173.
Hu, Y., and Fu, J., 1982, Micropalaeoflora from the Gaoshanhe Formation of late Precambrian of Luonan, Shaanxi and its stratigraphic significance: Bulletin of the Xi'an Institute of Geology and Mineral Resources, Chinese Academy of Geological Science, v. 4, p. 102–113.
Imachi, H., et al., 2020, Isolation of an archaeon at the prokaryote–eukaryote interface: Nature, v. 577, p. 519–525.
Inouye I., Hori, T., and Chihara, M., 1990, Absolute configuration of the flagellar apparatus of *Pterosperma cristatum* (Prasinophyceae) and consideration of its phylogenetic position: Journal of Phycology, v. 26, p. 329–344.
Jachowicz-Zdanowska, M., 2013, Cambrian phytoplankton of the Brunovistulicum: taxonomy and biostratigraphy: Polish Geological Institute Special Papers 28, 150 p.
Jankauskas, T.V., 1979, Middle Riphean microbiota of the southern Urals and the Ural region in Bashkiria: Proceeding of the USSR Academy of Sciences, v. 248, p. 190–193. [in Russian]
Jankauskas, T.V., 1980, Shisheniak microbiota of the Upper Riphean of the Southern Urals: Akademiya Nauka SSSR Transactions, v. 251, p. 190–192. [in Russian]
Jankauskas, T.V., 1982, Microfossils of the Riphean of the South Urals, the Riphean Stratotype, Paleontology, Paleomagnitism: Proceeding of the USSR Academy of Sciences, v. 268, p. 84–120. [in Russian]
Jankauskas, T.V., Mikhailova, N.S., and Hermann, T.N., 1989, Microfossils of the Precambrian of the USSR: Leningrad, Nauka. [in Russian]
Javaux, E.J., 2007, The early eukaryotic fossil record, *in* Jékely, G., ed., Eukaryotic Membranes and Cytoskeleton. Advances in Experimental Medicine and Biology, v. 607: New York, Springer, p. 1–19.
Javaux, E.J., 2011, Early eukaryotes in Precambrian oceans: Origins and Evolution of Life, v. 6, p. 414–449.
Javaux, E.J., 2019, Challenges in evidencing the earliest traces of life: Nature, v. 572, p. 451–460.
Javaux, E.J., and Knoll, A.H., 2017, Micropaleontology of the lower Mesoproterozoic Roper Group, Australia, and implications for early eukaryotic evolution: Journal of Paleontology, v. 91, p. 199–229.
Javaux, E.J., and Lepot, K., 2018, The Paleoproterozoic fossil record: implications for the evolution of the biosphere during Earth's middle-age: Earth-Science Reviews, v. 176, p. 68–86.
Javaux, E.J., and Marshal, C.P., 2006, A new approach in deciphering early protist paleobiology and evolution: combined microscopy and microchemistry of single Proterozoic acritarchs: Review of Palaeobotany and Palynology, v. 139, p. 1–15.
Javaux, E.J., Knoll, A.H., and Walter, M.R., 2001, Morphological and ecological complexity in early eukaryotic ecosystems: Nature, v. 412, p. 66–69.
Javaux, E.J., Knoll, A.H., and Walter, M., 2003, Recognizing and interpreting the fossils of early eukaryotes: Origins of Life and Evolution of the Biosphere, v. 33, p. 75–94.
Javaux, E.J., Knoll, A.H., and Walter, M.R., 2004, TEM evidence for eukaryotic diversity in mid-Proterozoic oceans: Geobiology, v. 2, p. 121–132.

https://doi.org/10.1017/jpa.2021.45 Published online by Cambridge University Press

Javaux, E.J., Marshall, C.P., and Bekker, A., 2010, Organic-walled microfossils in 3.2-billion-year-old shallow-marine siliciclastic deposits: Nature, v. 463, p. 934–938.
Kerans, C., 1982, Sedimentology and stratigraphy of the Dismal Lakes Group, Proterozoic, Northwest Territories [Ph.D. thesis]: Ottawa, Carleton University, 466 p.
Kerans, C., 1983, Timing of emplacement of the Muskox intrusion: constraints from Coppermine homocline cover strata: Canadian Journal of Earth Sciences, v. 20, p. 673–683.
Kerans, C., Ross, G.M., Donaldson, J.A., Geldsetzer, H.J., and Campbell, F.H.A., 1981, Tectonism and depositional history of the Helikian Hornby Bay and Dismal Lakes groups, District of Mackenzie, *in* Campbell, F.H.A., ed., Proterozoic Basin of Canada: Geological Survey of Canada Paper 81–10, p. 157–182.
Knoll, A.H., 2014, Paleobiological perspectives on early eukaryotic evolution: Cold Spring Harbor Perspectives in Biology, v. 6, a016121.
Knoll, A.H., and Lahr, D.J.G., 2016, Fossils, feeding, and the evolution of complex multicellularity, *in* Niklas, K.J., and Newman, S.A., eds., Multicellularity: Origin and Evolution: Cambridge, Massachusetts, MIT Press, p. 3–16.
Knoll, A.H., Swett, K., and Mark, J., 1991, Paleobiology of a Neoproterozoic tidal flat/lagoonal complex: the Draken Conglomerate Formation, Spitsbergen: Journal of Paleontology, v. 65, p. 531–570.
Knoll, A.H., Javaux, E.J., Hewitt, D., and Cohen, P., 2006, Eukaryotic organisms in Proterozoic oceans: Philosophical Transactions of the Royal Society B: Biological Sciences, v. 361, p. 1023–1038.
Koonin, E.V., 2010, The origin and early evolution of eukaryotes in the light of phylogenomics: Genome Biology, v. 11, art. 209.
Koumandou, V.L., Wickstead, B., Ginger, M.L., Van Der Giezen, M., Dacks, J.B., and Field, M.C., 2013, Molecular paleontology and complexity in the last eukaryotic common ancestor: Critical Reviews in Biochemistry and Molecular Biology, v. 48, p. 373–396.
Lamb, D.M., Awramik, S.M., Chapman, D.J., and Zhu, S., 2009, Evidence for eukaryotic diversification in the ~1800 million-year-old Changzhougou Formation, North China: Precambrian Research, v. 173, p. 93–104.
LeCheminant, A.N., and Heaman, L.M., 1989, Mackenzie igneous events, Canada: middle Proterozoic hotspot magmatism associated with ocean opening: Earth and Planetary Science Letters, v. 96, p. 38–48.
Li, G., Pang, K., Chen, L., Zhou, G., Han, C., Yang, L., and Wang, W., 2019, Organic-walled microfossils from the Tonian Tongjiazhuang Formation of the Tumen Group in western Shandong, North China Craton and their biostratigraphic significance: Gondwana Research, v. 76, p. 260–289.
Li, M., Liu, P., Yin, C., Tang, F., Gao, L., and Chen, S., 2012, Acritarchs from the Baicaoping Formation (Ruyang Group) of Henan: Acta Palaeontological Sinica, v. 51, p. 76–87.
López-García, P., and Moreira, D., 2015, Open questions on the origin of eukaryotes: Trends in Ecology and Evolution, v. 30, p. 697–708.
Loron, C.C., and Moczydłowska, M., 2018, Tonian (Neoproterozoic) eukaryotic and prokaryotic organic-walled microfossils from the upper Visingsö Group, Sweden: Palynology, v. 42, p. 220–254.
Loron, C.C., Rainbird, R.H., Turner, E.C., Greenman, J.W., and Javaux, E.J., 2018, Implications of selective predation on the macroevolution of eukaryotes: evidence from Arctic Canada: Emerging Topics in Life Sciences, v. 2, p. 247–255.
Loron, C.C., Rainbird, R.H., Turner, E.C., Greenman, J.W., and Javaux, E.J., 2019a, Organic-walled microfossils from the late Mesoproterozoic to early Neoproterozoic lower Shaler Supergroup (Arctic Canada): diversity and biostratigraphic significance: Precambrian Research, v. 321, p. 349–374.
Loron, C.C., François, C., Rainbird, R.H., Turner, E.C., Borensztajn, S., and Javaux, E.J., 2019b, Early fungi from the Proterozoic era in Arctic Canada: Nature, v. 570, p. 232–235.
Luo, Q.L., 1991, New data on the microplants from Changlongshan Formation of upper Precambrian in western Yanshan Range: Tianjin Institute of Geology and Mineral Resources, Bulletin 25, p. 107–118. [in Chinese with English abstract]
Mackie, R.A., Scoates, J.S., and Weis, D., 2009, Age and Nd–Hf isotopic constraints on the origin of marginal rocks from the Muskox layered intrusion (Nunavut, Canada) and implications for the evolution of the 1.27 Ga Mackenzie large igneous province: Precambrian Research, v. 172, p. 46–66.
Maithy, P.K., 1975, Micro-organisms from the Bushimay System (late Precambrian) of Kanshi, Zaire: The Palaeobotanist, v. 22, p. 133–149.
Marshall, C.P., Javaux, E.J., Knoll, A.H., and Walter, M.R., 2005, Combined micro-Fourier transform infrared (FTIR) spectroscopy and micro-Raman spectroscopy of Proterozoic acritarchs: a new approach to Palaeobiology: Precambrian Research, v. 138, p. 208–224.
Martí Mus, M., Moczydłowska, M., and Knoll, A.H., 2020, Morphologically diverse vase-shaped microfossils from the Russøya Member, Elbobreen Formation, in Spitsbergen: Precambrian Research, v. 350, art. 105899.
Miao, L., Moczydłowska, M., Zhu, S., and Zhu, M., 2019, New record of organic-walled, morphologically distinct microfossils from the late Paleoproterozoic Changcheng Group in the Yanshan Range, North China: Precambrian Research, v. 321, p. 172–198.
Mikhailova, N.S., 1986, New finds of microphytofossils from upper Riphean deposits of the Krasnoyar region, *in* Sokolov, B.S., ed., Current Questions of Contemporary Palaeoalgology: Kiev, Naukova Dumka, p. 31–37. [in Russian]
Moczydłowska, M., 2016, Algal affinities of Ediacaran and Cambrian organic-walled microfossils with internal reproductive bodies: Tanarium and other morphotypes: Palynology, v. 40, p. 83–121.
Moczydłowska, M., and Willman, S., 2009, Ultrastructure of cell walls in ancient microfossils as a proxy to their biological affinities: Precambrian Research, v. 173, p. 27–38.
Moczydłowska, M., Landing, E., Zang, W., and Palacios, T., 2011, Proterozoic phytoplankton and timing of Chlorophyte algae origins: Palaeontology, v. 54, p. 721–733.
Morais, L., Fairchild, T.R., Lahr, D.J.G., Rudnitzki, I.D., Schopf, J.W., Garcia, A.K., Kudryavtsev, A.B., and Romero, G.R., 2017, Carbonaceous and siliceous Neoproterozoic vase-shaped microfossils (Urucum Formation, Brazil) and the question of early protistan biomineralization: Journal of Paleontology, v. 91, p. 393–406.
Nagovitsin, K., 2009, Tappania-bearing association of the Siberian platform: biodiversity, stratigraphic position and geochronological constraints: Precambrian Research, v. 173, p. 137–145.
Nagy, R.M., Porter, S.M., Dehler, C.M., and Shen, Y., 2009, Biotic turnover driven by eutrophication before the Sturtian low-latitude glaciation: Nature Geoscience, v. 2, p. 415–418.
Naumova, S.N., 1949, Spores from the lower Cambrian: Proceeding of the USSR Academy of Sciences, v. 4, p. 49–56.
Pang, K., Tang, Q., Yuan, X.L., Wan, B., and Xiao, S., 2015, A biomechanical analysis of the early eukaryotic fossil *Valeria* and new occurrence of organic-walled microfossils from the Paleo-Mesoproterozoic Ruyang Group: Palaeoworld, v. 24, p. 251–262.
Parfrey, L.W, Lahr, D.J.G., Knoll, A.H., and Katz, L.A., 2011, Estimating the timing of early eukaryotic diversification with multigene molecular clocks: Proceedings of the National Academy of Sciences, v. 108, p. 13624–13629.
Parke, M., Boalch, G.T., Jowett, R., and Harbour, D.S., 1978, The genus *Pterosperma* (Prasinophyceae): species with a single equatorial ala: Journal of the Marine Biological Association of the United Kingdom, v. 58, p. 239–276.
Playford G., 2003, Acritarch and Prasinophyte Phycomata: A Short Course: Dallas, American Association of Stratigraphic Palynologists Foundation, 46 p.
Porter, S.M., 2016, Tiny vampires in ancient seas: evidence for predation via perforation in fossils from the 780–740 million-year-old Chuar Group, Grand Canyon, USA: Proceedings of the Royal Society B: Biological Sciences, v. 283, 20160221.
Porter, S.M., 2020, Insights into eukaryogenesis from the fossil record: Interface Focus, v. 10, 20190105.
Porter, S.M., and Knoll, A. H., 2000, Testate amoebae in the Neoproterozoic Era: evidence from vase-shaped microfossils in the Chuar Group, Grand Canyon: Paleobiology, v. 26, p. 360–385.
Porter, S.M., and Riedman, L.A., 2016. Systematics of organic-walled microfossils from the ca. 780–740 Ma Chuar Group, Grand Canyon, Arizona: Journal of Paleontology, v. 90, p. 815–853.
Porter, S.M., Meisterfeld, R., and Knoll, A.H., 2003, Vase-shaped microfossils from the Neoproterozoic Chuar Group, Grand Canyon: a classification guided by modern testate amoebae: Journal of Paleontology, v. 77, p. 409–429.
Prasad, B., and Asher, R., 2001, Acritarch Biostratigraphy and Lithostratigraphic Classification of Proterozoic and Lower Paleozoic Sediments (Pre-unconformity Sequence) of Ganga Basin, India: Dehradun, India, Geoscience Research Group, 151 p.
Prasad, B., Uniyal, S.N., and Asher, R., 2005, Organic-walled microfossils from the Proterozoic Vindhyan Supergroup of Son Valley, Madhya Pradesh, India: Palaeobotanist, v. 54, p. 13–60.
Pyatiletov, V.G., 1980, O nakhodkakh mikrofossilii roda *Navifusa* v Lakhandinskoi Svite [On the discovery of microfossils in the genus *Navifusa* in the Lakhanda Formation]: Paleontologicheskiy Zhurnal, v. 1980, p. 143–145. [in Russian]
Rainbird, R.H., Rooney, A.D., Creaser, R.A., and Skulski, T., 2020, Shale and pyrite Re–Os ages from the Hornby Bay and Amundsen basins provide new chronological markers for Mesoproterozoic stratigraphic successions of northern Canada: Earth and Planetary Science Letters, v. 548, 116492.
Ray, J.S., 2006, Age of the Vindhyan Supergroup: a review of recent findings: Journal of Earth System Science, v. 115, p.149–160.
Riedman, L.A., and Porter, S., 2016, Organic-walled microfossils of the mid-Neoproterozoic Alinya Formation, Officer Basin, Australia: Journal of Paleontology, v. 90, p. 854–887.

https://doi.org/10.1017/jpa.2021.45 Published online by Cambridge University Press

Riedman, L.A., and Sadler, P.M., 2017, Global species richness record and biostratigraphic potential of early to middle Neoproterozoic eukaryote fossils: Precambrian Research, v. 319, p. 6–18.
Riedman, L.A., Porter, S.M., and Calver, C.R., 2018, Vase-shaped microfossil biostratigraphy with new data from Tasmania, Svalbard, Greenland, Sweden and the Yukon: Precambrian Research, v. 319, p. 19–36.
Ross, G.M., Kerans, C., and Narraway, J.D., 1989, Geology, Hornby Bay and Dismal Lakes Groups, Coppermine Homocline, District of Mackenzie, Northwest Territories: Geological Survey of Canada, "A" Series Map 1663A, 1 sheet, https://doi.org/10.4095/128004
Samuelsson, J., Dawes, P.R., and Vidal, G., 1999, Organic-walled microfossils from the Proterozoic Thule Supergroup, northwest Greenland: Precambrian Research, v. 96, p. 1–23.
Schopf, J.W., 1968, Microflora of the Bitter Springs Formation, late Precambrian, central Australia: Journal of Paleontology, v. 42, p. 651–688.
Skulski, T., Rainbird, R.H., Turner, E.C., Meek, R., Ielpi, A., Halverson, G.P., Davis, W.J., Mercadier, J., Girard, E., and Loron, C.C., 2018, Bedrock geology of the Dismal Lakes–lower Coppermine River area, Nunavut and Northwest Territories: GEM-2 Coppermine River Transect, report of activities 2017–2018: Geological Survey of Canada Open File 8522, 39 p.
Talyzina, N.M., and Moczydlowska, M., 2000, Morphological and ultrastructural studies of some acritarchs from the lower Cambrian Lukati Formation, Estonia: Review of Palaeobotany and Palynology, v. 112, p. 1–21.
Tang, Q., Pang, K., Xiao, S., Yuan, X., Ou, Z., and Wan, B., 2013, Organic-walled microfossils from the early Neoproterozoic Liulaobei Formation in the Huainan region of North China and their biostratigraphic significance: Precambrian Research, v. 236, p. 157–181.
Tang, Q., Pang, K., Yuan, X., Wan, B., and Xiao, S., 2015, Organic-walled microfossils from the Tonian Gouhou Formation, Huaibei region, North China Craton, and their biostratigraphic implications: Precambrian Research, v. 266, p. 296–318.
Tang, Q., Hughes, N.C., McKenzie, N.R., Myrow, P.M., and Xiao, S., 2017, Late Mesoproterozoic–early Neoproterozoic organic-walled microfossils from the Madhubani Group of the Ganga Valley, northern India: Palaeontology, v. 60, p. 869–891.
Tang, Q., Pang, K., Yuan, X., and Xiao, S., 2020, A one-billion-year-old multicellular chlorophyte: Nature Ecology and Evolution, v. 4, p. 543–549.
Tappan, H.N., 1980, The Paleobiology of Plant Protists: New York, W.H. Freeman, 1028 p.
Timofeev, B.V., 1966, Micropaleophytological Investigations of Ancient Formations: Moscow, Nauka, 238 p. [in Russian]
Timofeev, B.V., 1969, Proterozoic Spheromorphida: Leningrad, Nauka. [in Russian]
Vidal, G., Siedlecka, A., 1983, Planktonic, acid-resistant microfossils from the upper Proterozoic strata of the Barents Sea region of Varanger Peninsula, East Finnmark, northern Norway: Norges Geologiske Undersøkelse NGU, v. 382, p. 45–79.
Vorob'eva, N.G., Sergeev, V.N., and Knoll, A.H., 2009, Neoproterozoic microfossils from the northeastern margin of the East European Platform: Journal of Paleontology, v. 83, p.161–196.
Vorob'eva, N.G., Sergeev, V.N., and Petrov, P.Y., 2015, Kotuikan Formation assemblage: a diverse organic-walled microbiota in the Mesoproterozoic Anabar succession, northern Siberia: Precambrian Research, v. 256, p. 201–222.
Turland, N.J., et al., 2018, International Code of Nomenclature for algae, fungi, and plants (Shenzhen Code) adopted by the Nineteenth International Botanical Congress Shenzhen, China, July 2017. Regnum Vegetabile 159: Glashütten, Koeltz Botanical Books, https://doi.org/10.12705/Code.2018
Waterbury, J.B., and Stanier, R.Y., 1978, Patterns of growth and development in pleurocapsalean cyanobacteria: Microbiological Reviews, v. 42, p. 2–44.
Weiss, A.F., 1984, Mikrofossilii iz verkhnego rifeya Turukhanskogo rajona [Microfossils from the Upper Riphean of the Turukhansk region]: Paleontologicheskiy Zhurnal, v. 2, p. 98–104. [in Russian]
Willison, J.H., and Brown, R.M., Jr., 1978, Cell wall structure and deposition in Glaucocystis: The Journal of Cell Biology, v. 77, p. 103–119.
Xing, Y.S., and Liu, K.C., 1973, On Sinian micro-flora in Yenliao region of China and its geological significance: Acta Geologica Sinica, v. 1, p. 1–64.
Yan, Y., and Zhu, S., 1992, Discovery of acanthomorphic acritarchs from the Baicaoping Formation in Yongji, Shanxi and its geological significance: Acta Micropalaeontologica Sinica, v. 9, p. 267–282.
Yin, L., 1987, Microbiotas of latest Precambrian sequences in China. Stratigraphy and palaeontology of systemic boundaries, *in* Nanjing Institute of Geology and Palaeontology Academia Sinica, ed., China: Precambrian-Cambrian Boundary: Nanjing, Nanjing Institute of Geology and Palaeontology Academia Sinica, p. 415–523.
Yin, L.M., 1997, Acanthomorphic acritarchs from Meso-Neoproterozoic shales of the Ruyang Group, Shanxi, China: Review of Palaeobotany and Palynology, v. 98, p. 15–25.
Yin, L., and Guan, B., 1999, Organic-walled microfossils of Neoproterozoic Dongjia Formation, Lushan County, Henan Province, North China: Precambrian Research, v. 94, p. 121–137.
Yin, L., Xunlai, Y., Fanwei, M., and Jie, H., 2005, Protists of the upper Mesoproterozoic Ruyang Group in Shanxi Province, China: Precambrian Research, v. 141, p. 49–66.

Accepted: 23 May 2021